Received: 27 March 2021 | Revised: 16 June 2021 | Accepted: 6 July 2021

DOI: 10.1111/ppl.13498

ECOPHYSIOLOGY, STRESS AND ADAPTATION

Physiologia Plantarum

The physiological acclimation and growth response of *Populus trichocarpa* to warming

J. Aaron Hogan[1,2] | Christopher Baraloto[1] | Cari Ficken[3] | Miranda D. Clark[4] | David J. Weston[4] | Jeffrey M. Warren[2]

[1]Department of Biological Sciences, Institute of Environment, Florida International University, Miami, Florida, USA

[2]Division of Environmental Science, Oak Ridge National Laboratory, Oak Ridge, Tennessee, USA

[3]Department of Geology, University at Buffalo, Buffalo, New York, USA

[4]Division of Biosciences, Oak Ridge National Laboratory, Oak Ridge, Tennessee, USA

Correspondence
J. Aaron Hogan, Department of Biological Sciences, Institute of Environment, Florida International University, Miami, FL, 33199 USA.
Email: jhogan@fiu.edu

Funding information
U.S. Department of Energy, Grant/Award Numbers: DE-AC05-1008 00OR22725, DE-SC0014664

Edited by: I. Ensminger

Abstract

Plant metabolic acclimation to thermal stress remains underrepresented in current global climate models. Gaps exist in our understanding of how metabolic processes (i.e., photosynthesis, respiration) acclimate over time and how aboveground versus belowground acclimation differs. We measured the thermal acclimation of *Populus trichocarpa*, *comparing* aboveground versus belowground physiology over time. Ninety genetically identical ramets were propagated in mesocosms that separated root and microbial components. After establishment at 25°C for 6 weeks, 60 clones were warmed +4 or +8°C and monitored for 10 weeks, measuring photosynthesis (A), leaf respiration (R), soil respiration (R_s), root plus soil respiration (R_{s+r}), and root respiration (R_r). We observed thermal acclimation in both A and R, with rates initially increasing, then declining as the thermal photosynthetic optimum (T_{opt}) and the temperature-sensitivity (Q_{10}) of respiration adjusted to warmer conditions. Photosynthetic acclimation was constructive, based on an increase in both T_{opt} and peak A. Belowground, R_{s+r} decreased linearly with warming, while R_s rates declined abruptly, then remained constant with additional warming. Plant biomass was greatest at +4°C, with 30% allocated belowground. Rates of mass-based R_r were similar among treatments; however, root nitrogen declined at +8°C leading to less mass nitrogen-based R_r in that treatment. The Q_{10}-temperature relationship of R_r was affected by warming, leading to differing values among treatments. Aboveground acclimation exceeded belowground acclimation, and plant nitrogen-use mediated the acclimatory response. Results suggest that moderate climate warming (+4°C) may lead to acclimation and increased plant biomass production but increases in production could be limited with severe warming (+8°C).

1 | INTRODUCTION

Surface temperatures of the Earth system continue to rise as anthropogenic climate change intensifies (Hansen et al. 2010). By 2100, global surface temperatures are predicted to be between 0.3 and 4.8°C higher than in 1850–1900, depending on the emissions scenario (IPCC 2014), with even greater increases at higher latitudes. Such widespread warming of the earth's terrestrial ecosystems,

including natural forests and agricultural forest plantations, will undoubtedly affect tree physiology, growth, and survival (Aitken et al. 2008; Allen et al. 2015). Although evidence for changes in tree growth rates and biomass production is mixed (Canham et al. 2018; McMahon et al. 2010; Peñuelas et al. 2011), some effects of increasing temperatures on tree physiology are already being observed. These include geographic range shifts (Monleon & Lintz 2015; Walther 2003), an increase in tree water use efficiency (Adams et al. 2020; Mathias & Thomas 2021), and changes in rates of photosynthesis and respiration (Dusenge et al. 2019; Kamarathunge et al. 2019). The degree of physiological plasticity to climate change within dominant tree genera, such as *Populus* is not well known, yet will affect carbon (C) and water fluxes at the ecosystem and global levels (King et al. 2006; Lombardozzi et al. 2015; Smith & Dukes 2013) and the provisioning of essential ecosystem services (e.g., net ecosystem exchange, tree plantation biomass production) in the future. Forest ecosystems and their dominant tree genera will have to either physiologically acclimate to warming or adapt in some way to increased temperatures; otherwise, they will face decline (Feeley et al. 2012).

Net C storage in the plant–soil system is the balance of aboveground plant metabolism (i.e., photosynthesis and respiration) and belowground plant and soil microbial respiration (i.e., C fixation vs. release; Luo 2007). Plant and soil metabolic processes have varying temperature-sensitivities. Warming has been shown to affect soil respiration rates (Bond-Lamberty & Thomson 2010), and both hetero- and autotrophic respiration are predicted to increase as the planet continues to warm (Atkin et al. 2005; Atkin & Tjoelker 2003; Bond-Lamberty & Thomson 2010). Photosynthesis, on the other hand, can acclimate (i.e., adjust to maintain or improve physiological functioning) to increasing temperature (Berry & Björkman 1980; Kamarathunge et al. 2018; Sage & Kubien 2007); but, there is little evidence that increases in photosynthetic rates with increasing temperature will keep pace with increases in respiration rates (Smith et al. 2020), especially if plants reach critical thermal thresholds. This mismatch could lead to an abrupt decline in C uptake and storage (Jump & Peñuelas 2005). To infer how continued warming will affect the ecosystem C balance of natural and agricultural systems, changes in whole plant physiology and their interaction with plant–soil feedbacks require greater understanding (Chapin III et al. 2009; García-Carreras et al. 2018).

Plant metabolism is the net sum of photosynthesis and respiration. Photosynthesis and respiration are complex biochemical processes that are highly enzyme-catalyzed, and thus temperature is a crucial factor that controls process rates (Bernacchi et al. 2003; Farquhar et al. 1980; Moore et al. 2021; Von Caemmerer 2000). Photosynthesis and respiration can both acclimate to increased temperature to some degree (Slot & Kitajima 2015; Slot & Winter 2016; Way & Yamori 2014), although the capacity for thermal acclimation has not been precisely quantified for many species. Photosynthetic acclimation is defined as any adjustments in leaf C assimilation that improve the plant's performance at higher temperatures (Slot & Winter 2016, Way & Yamori 2014). A *constructive* acclimatory response to increased temperature (*sensu* Way & Yamori 2014) increases both the temperature optimum of photosynthesis (T_{opt}) and the rate of photosynthesis at the growth temperature. Such a response demonstrates that leaf physiological adjustments (e.g., enzyme kinetics of Calvin cycle reactions) make the plant equally or better suited for carbon gain at the increased temperature. The increase in the rate of photosynthesis at the warmer temperature helps offset increases in respiration rates, which allows the plant to maintain a positive C balance. Internal leaf photosynthetic processes acclimate to temperature changes within days to weeks of temperature change (Berry & Björkman 1980; Yamori et al. 2014). The consensus for temperate trees is that T_{opt} can shift by one-third to half of the magnitude of change in mean daily air temperatures (i.e., there is an increase in T_{opt} of 0.4°C per degree change in air temperature; Kumarathunge et al. 2019; Sage & Kubien 2007; Yamori et al. 2014). However, the physiological cost of photosynthetic and respiratory acclimation on whole-plant carbon balance (e.g., biomass production, rates of root respiration) or whole-plant metabolism (e.g., nutrient use patterns) is less well understood.

Photosynthetic thermal acclimation is governed mainly by the temperature adjustment of three critical biochemical processes in the leaf: (1) the capacity of ribulose-1,5-bisphosphate carboxylase/oxygenase (Rubisco) to process (i.e., carboxylize) ribulose bisphosphate (RuBP), (2) the rate at which the Calvin cycle and light reactions can regenerate RuBP (i.e., RuBP regeneration), and (3) the capacity to regenerate organic phosphates for phosphorylation (i.e., triosephosphate use efficiency; Sage & Kubien 2007; Von Caemmerer 2000). Thus, RuBP carboxylation and regeneration are two of the three main biochemical processes that govern how photosynthetic rates acclimate to increased temperature (Berry & Björkman 1980; Von Caemmerer 2000). These processes are thought to dominate the biochemical adjustments that underlie acclimation under saturated light conditions and at ambient CO_2 levels (Sage & Kubien 2007). Also, according to Sharkey (2019), we may be misassigning the biochemical limitation of photosynthesis concerning RuBP carboxylation and regeneration and how these processes interact with triose phosphate limitation, which may or may not affect the up or down-regulation of CO_2 and RuBP limitation on assimilation (Rogers et al. 2020). At moderate temperature increases, RuBP-carboxylation limitation of photosynthesis is common, whereas RuBP regeneration becomes limiting at higher temperatures (Berry & Björkman 1980). Changes in the rates of RuBP carboxylation and regeneration, improved heat stability of Rubisco activase (Hikosaka et al. 2005; Sage & Kubien 2007; Yamori et al. 2006), and the regulation of the amount of RuBP and Rubisco in C_3 plant leaves are the main biochemical changes that drive acclimation of C_3 photosynthesis to increased temperatures (Crous et al. 2018; Scafaro et al. 2017). Because RuBP and Rubisco are nitrogen (N) rich, leaf N content serves as a good proxy for RuBP- and Rubisco-driven acclimation of photosynthesis to warming (Crous et al. 2018; Hikosaka 1997; Reich et al. 1998; Scafaro et al. 2017). Additionally, part of the acclimation of C_3 photosynthesis to increased temperatures is attributable to an increase in electron transport rates and temperature-related changes in the light reactions of photosynthesis (e.g., changes in J_{max} rates or

chlorophyll fluorescence, Yamasaki et al. 2002) if the heat stress is moderate and does not damage photosystems (Song et al. 2014).

Unlike photosynthesis, which occurs primarily in plant leaves, respiration occurs throughout the plant. Key metabolic processes, including cell growth, biomass maintenance, and ATP production, rely on cellular respiration. We know less about root respiration than that of leaves or stems. It is not entirely clear if acclimation of root metabolic processes coincides with the acclimation of photosynthesis. Root respiration, which generates the C compounds used for uptake in the roots (e.g., sugars–fructose, galactose; enzymes–amylase, phosphatase; and organic, phenolic or amino acids), represents a significant component of CO_2 loss in plants, with 8–52% of photosynthate being respired back through the roots (Lambers et al. 1996; Pregitzer et al. 1998). Over short time periods, root respiration has been shown to increase significantly in response to warming (Bryla et al. 2001; Wang et al. 2021). Rates of root respiration do acclimate to rising temperatures; however, it is predicted that roots have a lower capacity for physiological acclimation to increased temperatures than do leaves, either due to a lower degree of temperature sensitivity in cellular biochemical processes or to the temperature buffering capacity of the soil (Atkin et al. 2000; Eissenstat et al. 2013; Pregitzer et al. 2000). Studies that have measured respiratory acclimation of roots to increased temperature have not linked it to plant physiological or soil metabolic acclimation, thus the consequences of thermal acclimation in root respiration to plant–soil system functioning are not entirely understood.

The temperature sensitivity of root respiration has been shown to vary with root age, root order, and soil moisture (Atkin et al. 2000; Ceccon et al. 2016; Palta & Nobel 1989), with younger, more-hydrated roots having higher rates of respiration, which reflects greater metabolic activity (i.e., active nutrient uptake and root enzyme production). Additionally, if root respiration rates are related to root lifespan, warming could decrease root lifespan as respiration rates increase (Eissenstat et al. 2013). Using data from eight commonly studied taxa, Smith et al. (2019) reported that respiration rates of leaves and photosynthetic stems increased to a greater extent than roots following temperature increase, indicating that leaves and stems have greater thermal acclimation capacity than roots. A second recent study on the respiration rates of tropical seedlings of eight species (Noh et al. 2020) found no clear trend in root respiration in response to warming but reported that respiration rates were correlated with root N content, and that the temperature sensitivity of root respiration (Q_{10} R_r) was positively related to root tissue density. Many other studies have confirmed the relationship between root respiration and root tissue N content (Burton et al. 2002; Pregitzer et al. 1998; Pregitzer et al. 2000; Reich et al. 2008; Roumet et al. 2016). Few studies have compared the degree of acclimation of photosynthesis and respiration across plant organs and in relation to the plant–soil system over time, and few studies have related acclimatory differences to variation in plant biomass production with temperature.

To address the magnitude and time course of above versus belowground responses to thermal stress, we investigated the physiological acclimation of *Populus trichocarpa* Torr. & A.Gray ex Hook. (Salicaceae) to increased temperatures in a whole-plant warming experiment. Our experiment used a novel mesocosm methodology able to link plant acclimation to belowground carbon dioxide (CO_2) efflux. We used several routines for high-frequency leaf gas exchange measurements and belowground CO_2 efflux to compare aboveground versus belowground physiological acclimation of *P. trichocarpa*. Poplar trees have been shown to be able to acclimate to increased temperatures (Silim et al. 2010), with relatively consistent responses across genotypes (i.e., populations from differing geographic origins; Gornall & Guy 2007; Silim et al. 2010). Experiments that have investigated the thermal acclimation of poplar often rely on two measurements, pre- and post-warming. We sought to understand the time course of acclimation responses and how they compare among the different organs and thermal acclimation parameters because of the dynamic nature of temperature changes and the potential for source-sink imbalances above and belowground. We asked:

1. In *P. trichocarpa*, do rates of belowground (root and root plus soil) respiration acclimate to warming?
2. What is the time course of aboveground physiological acclimation to warming, and does belowground acclimation track aboveground acclimation?

We expected to find some degree of acclimation to warming in root respiration rates and root plus soil CO_2 efflux. Still, we hypothesized that root respiration would show less acclimation than leaf physiological acclimation (i.e., photosynthetic, and respiratory acclimation of leaves). Additionally, we hypothesized that that rate (i.e., time course) of aboveground acclimation would be faster with more warming and that belowground acclimation (i.e., root plus soil CO_2 efflux) should track aboveground acclimation.

2 | METHODS

2.1 | Experimental design—*P. trichocarpa* Clones & mesocosm growth boxes

Western black cottonwood (*Populus trichocarpa*) ramets of the Nisqually-1 genotype were obtained from the Joint Genome Institute (Walnut Creek Campus) in October 2018. Ramets were planted into leach tubes containing growth medium and allowed to establish for 10 weeks. The growth medium used throughout the experiment was a well-draining potting mix (pH 5.5–6.5), consisting of peat moss, vermiculite, perlite, and processed pine bark (Farfad 52 mix, SunGro Horticulture), mixed with time-release Osmocote Plus Fertilizer (0.7 g kg^{-1} 15-9-12, NPK). Ninety established clones with an average height of 14.4 cm (range: 8.1–24.8 cm) and average basal stem diameter of 4.5 mm (range: 2.9–6.5 mm) were transplanted from leach tubes into mesocosm growth boxes on 29 July 2019. Stems were trimmed at the seventh leaf node, and any roots extending beyond the bottom of the leach tube were cut off to standardize clone size prior to transplanting.

Mesocosm growth boxes (38 × 23.5 × 18 cm L × W × H, 15.14 L capacity) were constructed from AkroGrid containers (model 33,168, Akro-Mils), using a modified methodology of Ficken and Warren (2019). Three small holes were drilled on either side of the boxes, near the bottom, to allow for water drainage. Each box was filled with 3.5 kg. of potting mix (as described above; hereafter, soil) and had a 1-μ mesh partition installed to separate one-third of the box volume. The mesh barrier was designed to exclude plant roots but permit the movement of microbes and water between mesocosm portions, effectively creating a soil control for each mesocosm. *P. trichocarpa* clones were positioned in the middle of the larger compartment (one plant per container). Each compartment was equipped with a PVC soil CO_2-efflux collar. Collars were made from schedule 40 PVC (5 cm diameter and 10 cm in length), with twelve 3.7 cm diameter holes drilled into the collar portion that sat below the soil surface. Mesocosm boxes were encased in CoolShield thermal bubble wrap (ULINE) to mimic natural temperature differences between the soil and air.

2.2 | Experimental design—Growth conditions & temperature treatments

The duration of the experiment was 16 weeks. For an initial 6-week establishment period, all 90 of the plants were grown together in a climate-controlled greenhouse to allow them to establish root biomass in the mesocosms. During the initial establishment period, the plants were drip irrigated, receiving about 1 L of water per day. At weeks two and four, plants received two doses of soluble fertilizer (about 1.4 g fertilizer per dose delivered in approximately 1.5 L of water, Southern Ag Nitrate Special 20-10-20, NPK). When the plants were 44 days old, 60 of the plants were transferred to two walk-in growth chambers (30 per chamber, CONVIRON). Following this, plants were grown at experimental temperatures for 10 weeks. Throughout the experiment, axillary sprouts were pinched off by hand before development to constrict plant growth to the main stem.

The control environment for the experiment (i.e., ambient treatment) remained the greenhouse, and two separate growth chambers were used for the warming treatments. Growth chambers were set to 70% relative humidity, and at 29°C (i.e., a +4°C treatment) and 33°C (i.e., a +8°C treatment), respectively, each with a 4°C degree nighttime temperature drop (Table 1). Growth chamber conditions were matched to the environmental conditions of the greenhouse during the initial establishment period, where temperatures peaked at 25°C with at most a 4°C nighttime decrease. A climate station with two air thermometers, two relative humidity sensors, two quantum sensors, and 12 soil temperature sensors was used throughout the experiment and rotated among the three treatments at 2 week intervals to monitor environmental conditions.

The plants grew vigorously during the initial establishment period, on average >2 cm day^{-1} in height. They were 1.5–2 m in height when transferred to the growth chambers and reached the ceiling in the growth chambers about 3 weeks into warming treatments. Therefore, at week 10 (day 71) of the experiment, corresponding to the midpoint of the treatment portion of the experiment, all plants were cut to 1.5 m height. Trimmed biomass and leaf areas were measured and accounted for in the final biomass calculations. Additionally, at that time, the experimental treatments were swapped between growth chambers to spread any latent effects of each specific growth chamber equally over both treatments. During the last week of the experiment, mesocosm box water loss (i.e., due to evapotranspiration) was quantified by entirely watering each replicate, recording its weight at that time and again 24 h later.

2.3 | Aboveground acclimation to warming—measurements of leaf gas exchange & fitting of response curves

Poplars have indeterminate growth, meaning stems continuously elongate; moreover, they have leaf orthostichies (i.e., where eight leaves form a single growth unit and can share photosynthate; Larson & Isebrands 1971), so photosynthesis measurements were always conducted on a recently mature leaf located at the eighth-most terminal position (i.e., standardized by leaf plastochron index). All measurements

TABLE 1 Environmental conditions (light conditions, daytime and nighttime air and soil temperatures, relative humidity, and vapor pressure deficit) of the experimental treatments (mean values ± *SE*)

Treatment	Daytime air temperature (°C)	Nighttime air temperature (°C)	Relative humidity (%)	Daytime PAR (μmol m^{-2} s^{-1})	Daytime soil temperature (°C)	Nighttime soil temperature (°C)	Vapor pressure deficit (kPa)
Initial	23.95 ± 0.11^{B}	25.38 ± 0.23^{B}	69.90 ± 3.00^{B}	311.07 ± 16.87^{B}	24.61 ± 0.13^{B}	25.64 ± 0.32^{B}	1.024 ± 0.007^{A}
Ambient	21.55 ± 0.28^{A}	19.75 ± 0.38^{A}	58.28 ± 2.23^{A}	99.71 ± 15.39^{A}	20.81 ± 0.38^{A}	20.26 ± 0.81^{A}	1.081 ± 0.035^{A}
+4°C	29.33 ± 0.07^{C}	25.53 ± 0.27^{B}	72.53 ± 1.03^{B}	139.81 ± 9.21^{A}	26.69 ± 0.07^{C}	26.62 ± 0.13^{B}	1.102 ± 0.027^{A}
+8°C	32.91 ± 0.19^{D}	29.01 ± 0.07^{C}	67.45 ± 1.85^{B}	107.15 ± 9.04^{A}	29.94 ± 0.10^{D}	29.41 ± 0.18^{C}	1.303 ± 0.048^{B}
Treatment $F_{(3,103)}$	730.90***	269.60***	14.91***	54.62***	293.70***	107.60***	15.23***

Note: Data are from a meteorological station comprised of two air temperature, relative humidity, and light quantum sensors, and 12 soil temperature sensors. Data were collected at hourly intervals, and after experimental-warming initiated, the station was rotated throughout the treatment at roughly 2 week intervals. *F*-statistics are for analyses of variance in the form of: ~treatment. *F* probabilities are all statistically significant: ***$P < 0.001$. Letters denote statistical groupings from Tukey HSD post-hoc tests ($n = 107$).

were made using the Li-6800 portable photosynthesis system (Li-COR Inc). Criteria for assessing leaf stability in the photosynthesis system leaf chamber and logging data points was consistent throughout the experiment and across all measurements (see Table S1). To assess aboveground acclimation, we measured leaf photosynthesis over time using several measurement routines—survey measurements were done weekly at experimental conditions, and leaf gas exchange responses to temperature, CO_2 and light were done every 2 weeks.

First, survey measurements of coupled leaf gas exchange and chlorophyll fluorescence were done weekly on every plant in the experiment at treatment temperature. Chlorophyll fluorescence can help identify thermal stress responses of leaves, and classify light (i.e., photochemistry) versus Calvin cycle (i.e., biochemical) photosynthetic acclimation. Fluorometer parameters were consistent throughout and we utilized a pulse-modulated flash, followed by a dark pulse (see List S1 for Li-6800 fluorometer settings). For survey measurements, instrument settings were 1000 μmol m^{-2} s^{-1} light, 400 μmol mol^{-1} CO_2, 600 μmol s^{-1} flow rate, and the leaf chamber humidity was controlled to maintain leaf vapor pressure deficit (VPD) at 1.25 kPa. Controlling leaf chamber humidity to maintain leaf VPD at 1.25 kPa resulted in little to no change in leaf environmental conditions when taking gas exchange measurements (see Table 1 for environmental VPD).

Second, three types of leaf gas exchange response curves were measured—leaf photosynthesis and dark respiration responses to temperature, leaf photosynthesis-CO_2 responses and leaf photosynthesis-light responses. Response curves were conducted every 2 weeks on the same leaf for at least six plants per treatment. All response curve models were fitted separately for each leaf.

Leaf photosynthesis- and respiration-temperature response curves were measured across a temperature range of ±10°C from the growth environment temperature concurrently on the same leaf, one after another. While holding constant all other Li-6800 leaf chamber parameters (i.e., leaf VPD at 1.25 kPa), the air temperature was increased in 2°C increments (ranges: 18–42°C for the ambient treatment, 20–44°C for the +4°C treatment, and 24–48°C for the +8°C), with light at 1000 μmol m^{-2} s^{-1}. Maintaining VPD constant (rather than RH) reduces the confounding impact of VPD on measurements and helps isolate the response of photosynthesis to temperature alone. After completion of the photosynthetic temperature-response curve, we turned the actinic light off and waited for stability of leaf dark respiration. The dark respiration temperature response curve was initiated at this point to take advantage of the leaf already being acclimated to the high temperature. Once stable, we developed the response curve by progressively decreasing the leaf chamber temperature in 2°C increments, each time waiting for stability prior to recording the rate of leaf dark respiration. Each leaf gas exchange measurement (i.e., photosynthesis and respiration) was carefully observed and logged, and contingent on machine stability. Photosynthesis-temperature response curves were fit using a standard quadratic equation that modeled leaf photosynthesis (A) as a function of leaf temperature (T_{leaf}; as measured by the Li-COR thermocouple): $A = aT_{leaf} + bT_{leaf}{}^2 + c$. The R^2 values of fitted quadradit models were always >0.9 (and usually >0.95), negating the need to use a more sophisticated model (i.e., that of Cunningham & Read 2002). The temperature optimum of net photosynthesis (T_{opt}) and the rate of net photosynthesis at T_{opt} (A_{opt}) were determined via the T_{leaf} and A values at the maximum of the fitted curve, respectively. Leaf dark respiration-temperature response curves were fit using an exponential linear model: $\log R_d = aT_{leaf}$. Models were fit using the range of the measured data, roughly ±10°C from the growth environment temperature (see measurement temperature intervals by treatment above), and predicted from 16 to 47°C. Our leaf dark respiration-temperature data followed a typical Arrhenius-style exponential increase within our measurement range, and since we saw no evidence of a decline in leaf dark respiration at higher temperatures, we fit the simple exponential linear model instead of a more complex model (e.g., that of Heskel et al. 2016). The Q_{10} value of leaf dark respiration, or the magnitude of increase in leaf dark respiration for a 10°C increase in temperature, was calculated using the exponential function of the fitted model coefficient (i.e., slope parameter, α) times 10.

Leaf photosynthesis-CO_2 response curves were conducted at treatment temperatures using the traditional method, where all leaf chamber parameters were held constant, but the concentration of extracellular CO_2 was varied between 50 and 2000 μmol mol^{-1} in 13 steps. The Farquhar-Berry-von Caemmerer model (Farquhar et al. 1980) was fit to the CO_2 response data using the "plantecophys" package (Duursma 2015) in R v.3.6.1 (R Core Team 2019), which derives temperature-standardized estimates (at 25°C) of the maximum velocity of carboxylation ($V_{cmax,25}$) and the maximum rate of electron transport ($J_{max,25}$) from the fitted curves.

In order to confirm that light sensitivity was not a confounding factor in our experiment, we measured light response curves throughout the experiment at the same interval and on the same leaves as the temperature- and CO_2-response curves. Light curves were assembled at treatment temperatures from high to low light intensity, decreasing light from 2000 to 0 μmol m^{-2} s^{-1} in 15 steps. Light response curve parameters were estimated using non-linear regression of a non-rectangular parabola (Marshall & Biscoe 1980) in the form of: $A_{net} = \frac{\Phi \mathrm{PPFD} + \sqrt{(\Phi \mathrm{PPFD} + A_{max})^2 - 4\theta\Phi PPFD + A_{max}}}{2\theta} - R_d$, where A_{net} and A_{max} are net and maximum (area-based) rates of photosynthesis, respectively, $PPFD$ is light intensity, Φ is the apparent quantum yield, R_d, is leaf dark respiration, and θ is the dimensionless curvature parameter. From fitted light-response curves, estimates of the light compensation point (I_{comp}) and the light saturation point at 75% of A_{max} ($I_{sat(75)}$) were computed. Code was used from Heberling and Fridley (2013).

2.4 | Measurement of leaf functional traits

Leaf morphology and tissue nutrient concentration were also always measured on the eighth-most terminal leaf. Leaf areas where the Li-6800 was attached were sampled immediately after photosynthetic responses were measured. Specific leaf area (SLA) and leaf N content

were assessed using the leaf punch method, where six circular leaf discs (Ø 18.5 mm) were punched out from the leaf tissue area where the Li-6800 was clamped to measure photosynthetic responses (to CO_2, light, and temperature). SLA was averaged across all six discs, and discs were homogenized into one sample for elemental analysis. Leaf C and N content were measured using a Carlo Erba NA 1500 Elemental Analyzer (Thermo Scientific) at the Duke Environmental Stable Isotope Laboratory in Durham, North Carolina.

2.5 | Belowground acclimation to warming—measurements of belowground CO_2 flux, root respiration, and their temperature sensitivities

Measurements of belowground soil CO_2 efflux (R_{BG}) were conducted weekly and separately for both (i.e., soil and soil with plant root) compartments of each mesocosm using an Li-6252 IRGA (Li-COR Inc.) set up to detect small volume CO_2 gas injections. PVC collars were capped with PVC caps fitted with 20 mm butyl septa. When capping collars, a needle was used to vent the collar headspace (volume of 196 cm^3) to avoid changes in air pressure. Headspace air was mixed by pumping 3 × 50 ml syringe. The needle was removed from the septum, and a 1-mL air sample was drawn from the headspace and immediately injected into the IRGA setup. An N_2 carrier gas at 0.1 L min^{-1} flowrate carried the air sample to the IRGA, where IRGA integration values (maximum and total integrated area) were recorded over a 15-second interval from the time of injection. PVC collars were left capped to incubate for at least 1 h and resampled. To minimize diel variation in soil respiration and to standardize soil moisture effects, we sampled mesocosms and their respiration chambers at roughly the same time of day and in the same order for all dates. For each sampling run, we used four CO_2 gas standards (100, 500, 1000, and 1600 ppm) to create a standard curve using least-squares regression, with which we calculated headspace sample CO_2 concentrations using their IRGA integration values. Differences in CO_2 concentrations over incubation time were converted to R_{BG} rates using chamber volume and area.

To measure the temperature sensitivity of belowground CO_2 flux, we conducted whole-plant temperature responses using the growth chambers. Five plants from each treatment were selected, placed in the growth chamber, and allowed to acclimate overnight to 15°C. Over the period of 1 day, the temperature of the growth chamber was varied from 15 to 35°C at a rate of 5°C increase every 2 h. Plants were allowed to acclimate for about 45 min as temperature increased, and then measurements of rates of belowground CO_2 flux (for both soil and soil + root mesocosm compartments, as described above) were conducted, incubating the PVC belowground respiration chambers for at least an hour. The climate station was used throughout to monitor air and soil temperatures. Ordinary least-squares linear regressions were fitted to the soil and soil + root measurements by treatment ($n = 25$ for each compartment per treatment). The temperature sensitivity of belowground CO_2 flux was determined using the following equation, based on the linear regression fits: $Q_{10} = \left(\frac{R_2}{R_1}\right)^{10°C/(T_2-T_1)}$.

At the end of the experiment (on day 86 and 101, which was 42 and 57 days after warming began), root respiration (R_r)-temperature response curves were conducted on six plants per treatment. About 60 g (range 40–79 g) of fresh fine root biomass was placed in a Walz 3010-GWK1 gas exchange chamber (Heinz Walz GmbH), fitted to a Li-6800 IRGA (Li-COR Inc.) and rates of R_r were measured from 15 to 50°C in 2.5°C increments. The Walz 3010-GWK1 gas exchange chamber permits precise temperature control using the GFS-Win software. Following gas-exchange measurements, root biomass was dried and weighed, and root respiration measurements were standardized by the amount of dry root biomass present in the chamber (range: 4–10 g). The temperature response of R_r was modeled using non-linear least-squares regression in the form of: $R_T = R_0(c - bT)^{T/10}$, where R_T is R_r at a given temperature, T, R_0 is the root respiration rate at 0°C, and b and c are constants that describe the slope and intercept of the Q_{10} versus T relationship of R_r (Atkin et al. 2000; Atkin et al. 2005; Palta & Nobel 1989). The root respiration-temperature relationship is not constant with increasing temperature (i.e., the slope of the Q_{10}-T relationship varies with T, Atkin et al. 2000). The Q_{10} value for R_r at each temperature can be calculated via the slope of (i.e., differentiating) the R_r-T relationship. Accordingly, a third-order polynomial linear regression was fitted to log-transformed R_r data in relation to T, and the derivative of the fitted curve was taken at each measurement T (Q_{10} R_r). We also differentiated the models at 29°C (an intermediate temperature) to compare Q_{10} R_r at a standard temperature. Lastly, the R_r Q_{10}-T relationship was modeled using a quadratic curve.

2.6 | Quantifying plant growth and biomass production

Repeated stem basal diameter and plant height measurements were made using a digital Vernier caliper (0.1 mm precision) and tape measure (to the nearest 0.1 cm), respectively. Stem basal diameter and plant height measurements were conducted when clones were planted in the mesocosms, when plants were moved to the warming treatments (day 44), just after plants were trimmed (day 72), and when the experiment concluded (day 118). Plants were harvested at various intervals, on average, every 3 weeks to quantify whole plant biomass over time, compare among treatments and collect leaf and root tissue samples, however we only use growth and biomass from plants that grew to the end of the experiment for statistical analyses ($n = 51$, 17 plants per treatment in a balanced design). Upon harvesting, whole-plant leaf area was estimated by scanning all plant leaves through a Li-3100 Area Meter (Li-COR Inc.). For plant biomass measurements, plant material was dried at 70°C in an oven for several days, until constant mass, then weighed. The height and biomass of plants that were removed because of trimming were quantified and incorporated into all calculations.

2.7 | Statistical analyses

Environmental conditions of the treatments were statistically compared using a one-way analysis of variance (ANOVA), where treatment was the dependent variable, followed by the post-hoc Tukey test for honest significant differences (HSD).

For measured leaf gas exchange rates or related model-derived parameters from photosynthetic or respiratory response curves, we used a two-way ANOVA in the form of y ~ treatment × time. This statistically tests for differences in the physiological acclimation to temperature among treatments, and time, including the interaction between treatment and time. We examined if a repeated-measure error term greatly affected ANOVA inference; the statistics changed little, indicating a weak or only partial correlation between samples within each treatment over time. Potentially, randomly selecting plants helped limit the correlation. However, for most (i.e., 4 of 7) of the parameters, the interaction of treatment and time was significant. Therefore, we elected to fit ANOVA models (in the form of y ~ treatment) separately for each time period. ANOVA statistics were Bonferroni corrected to account for multiple comparisons over time. Similarly, within each time period, Tukey HSD post-hoc tests were applied to determine which treatments were statistically different from one another. This same procedure was applied to the leaf functional trait measurements that accompanied the photosynthetic or respiratory response curves.

For the chamber-based measurements of R_{BG}, we used a linear mixed-effects model (LMM). The data were verified to adhere to normality, and the model was fit using data from the 10 weeks of experimental warming (excluding measurements during the initial phase, where plants were establishing root biomass in the mesocosms). Based on the design, a random intercept term was justifiable for each mesocosm containing a single plant with two chambers (root + soil and soil only). Fixed effects for time, chamber, and treatment, including all interactions, were considered. The best fitting LMM was selected based on AIC using model backward selection via the step function in the 'LmerTest' package (Bates et al. 2015; Kuznetsova et al. 2017), which backward selects random effects then fixed effects. All model diagnostics were verified, effects were estimated using restricted maximum likelihood, and the model was visualized and interpreted with tools from the 'sjPlot' package. The temperature sensitivity of belowground respiration (i.e., Q_{10} of R_{BG}) was compared with a two-way ANOVA (treatment × time) followed by Tukey HDS post-hoc test for treatment.

For R_r measurements (both mass-based and mass N-based rates) and their temperature sensitivity, we grouped all measurements together and compared treatments using a one-way ANOVA, where treatment was the dependent variable. Similarly, plant growth and biomass data for plants grown from the start to the end of the experiment were analyzed using a one-way ANOVA, which tested for treatment differences. Treatments were compared using Tukey post-hoc HSD tests.

All analyses were done in R v.3.6.1 (R Core Team 2019), and all the ANOVAs were conducted using the 'aov' function in the base package in R. All statistical analyses are shown in Appendix S2. Throughout the results, mean values ± standard errors are presented (unless otherwise specified). Examples of code used to run all analyses can be found in Appendix S3.

3 | RESULTS

Using two walk-in growth chambers to raise the temperature to roughly +4 and +8°C from ambient temperature, and a greenhouse for the ambient temperature treatment (i.e., control), the implemented temperature treatments created consistent differences in air and soil temperatures among growth environments (Table 1). Although closer to 25°C at the start of the experiment, the temperature dropped slightly to around 21°C in the ambient treatment as the experiment progressed. Small differences in growing environment vapor pressure deficit (VPD) were recorded; however, environmental VPD was always between 1 and 1.3 kPa, even for the warmest treatment. All of the environmental variables in Table 1 (i.e., daytime air temperature, nighttime air temperature, air relative humidity, daytime photosynthetically active radiation, daytime soil temperature, nighttime soil temperature, and VPD) differed across treatments. Water losses due to evaporation and transpiration from mesocosms (measured on the last day of the experiment) were 1.29 ± 0.01 L day^{-1} in the ambient treatment, 1.81 ± 0.02 L day^{-1} in the +4°C treatment, and 2.23 ± 0.02 L day^{-1} in the +8°C treatment. Therefore, mesocosms in +4°C and + 8°C treatments lost 41% and 73% more water, respectively, than mesocosms at ambient conditions ($F_{(2,48)} = 43.99$, $P < 0.001$).

3.1 | Leaf photosynthetic acclimation

During the initial establishment period, rates of A and g_{sw} averaged 20.2 (± 0.1) μmol m^{-2} s^{-1} and 0.47 (±0.01) mol m^{-2} s^{-1}, respectively (Figure 1A,B). Following their introduction to the warming treatments, survey measurements of A (at treatment air temperatures) diverged among treatments, increasing slightly in the warming treatments but continuing to decline slightly in the ambient treatment (Figure 1A). A was statistically different among treatments ($F_{(2,636)} = 79.212$, $P \ll 0.001$) and over time (see Appendix S2 for complete ANOVA result). Treatment differences in A persisted for the first 7 weeks of warming, then became statistically similar (Appendix S2). After 10 weeks of warming, A averaged 13.9 (± 0.9) μmol m^{-2} s^{-1} for ambient treatment and 13.8 (±0.6) and 12.5 (±0.7) μmol m^{-2} s^{-1} for plants in the +4 and +8°C treatments, respectively (Figure 1A). Rates of g_{sw} initially decreased in the warmed treatments relative to the ambient treatment during the first week of warming but then roughly mirrored patterns in A (Figure 1B). Over the entire experiment, g_{sw} differed significantly among treatments ($F_{(2,636)} = 111.41$, $P \ll 0.001$) with g_{sw} in the ambient treatment (0.461 ± 0.01 mol m^{-2} s^{-1}) being significantly lower than the warming treatments (0.561 ± 0.01 mol m^{-2} s^{-1} for the +4°C treatment and 0.572 ± 0.01 mol m^{-2} s^{-1} for the +8°C

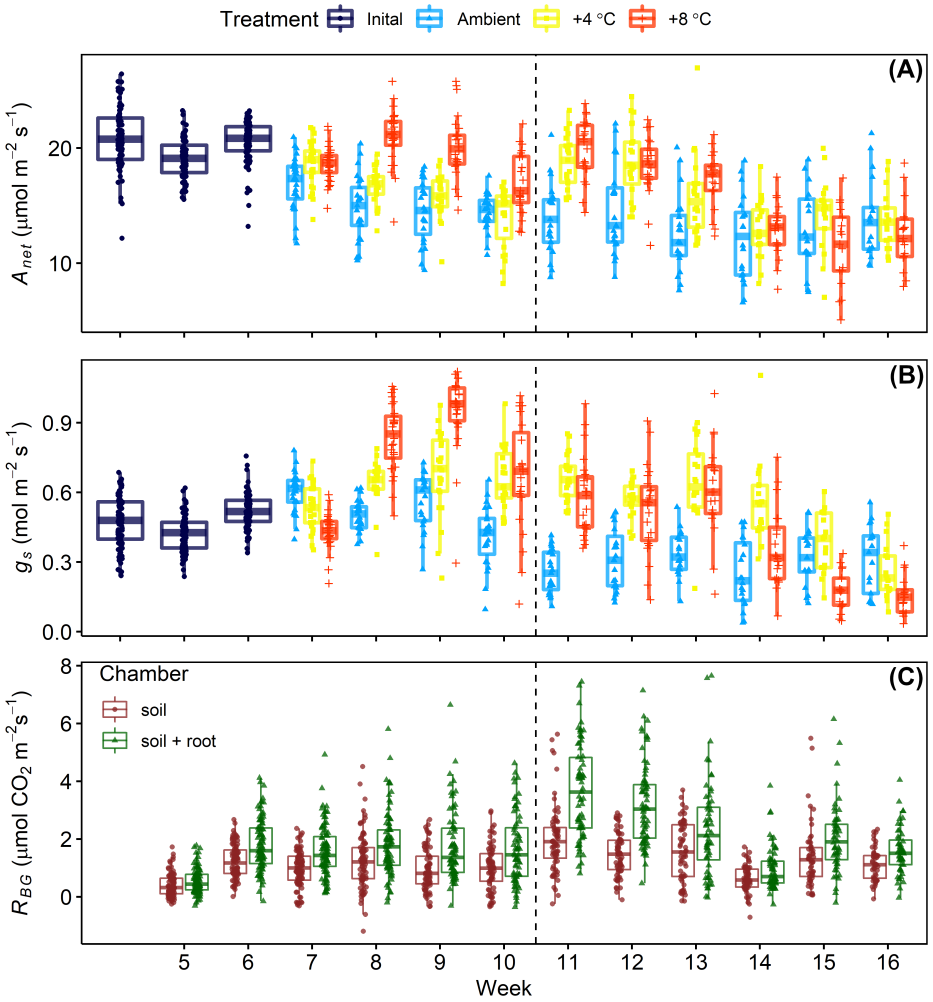

FIGURE 1 (A) Measurements of maximum leaf net photosynthetic rates (A_{net}, in micromoles CO_2 per square meter leaf area per second), (B) stomatal conductance to water vapor (g_{sw}, in moles per square meter leaf area per second) and (C) belowground respiration (R_{BG}, for respiration collars containing soil only and soil with roots in micromoles CO_2 per square meter soil area per second) for experimentally warmed *P. trichocarpa* clones. Temperature treatments were applied from week 7. The vertical dotted line denotes when plants were trimmed at day 71

treatment), which were statistically equivalent. After 10 weeks of warming, g_{sw} averaged 0.313 (±0.04) mol m^{-2} s^{-1} for the ambient treatment and 0.262 (±0.03) and 0.160 (±0.02) mol m^{-2} s^{-1} for the +4 and +8°C treatments, respectively (Figure 1B). At this time, differences in g_{sw} were still statistically significant ($F_{(2,48)} = 7.03$, $P < 0.01$), being about 0.1 mol m^{-2} s^{-1} and 0.15 mol m^{-2} s^{-1} lower in the 8°C treatment, relative to the +4°C and ambient treatment, respectively (Figure 1B).

Chlorophyll fluorescence measurements tracked the acclimation of the photosynthetic light reactions to increased temperature. The chlorophyll fluorescence ratio (F_v'/F_m') averaged 0.657 ± 0.006 in week 6 in the initial greenhouse conditions, increased slightly as plants matured to maximize at 0.670 ± 0.005 at week 9 (3 weeks after warming initiated), then decreased over time (average F_v'/F_m' at week 16 was 0.538 ± 0.01 across all treatments, Figure S1A). F_v'/F_m' was statistically different over time ($F_{(9,636)} = 23.838$, $P < 0.001$) and among treatments ($F_{(2,636)} = 4.862$, $P < 0.01$), with a significant interaction between treatment and time (Appendix S2). The other notable differences in leaf chlorophyll fluorescence among treatments were in the quantum efficiency of photosystem II (Φ_{PSII}, Figure S1B), the quantum yield of CO_2 assimilation corrected for dark respiration (Φ_{CO2}, Figure S1C), the quantum yield of non-photochemical quenching (Φ_{NPQ}, Figure S1D), and fluorometer-estimated electron transport rate of photosystem II (ETR_{PSII}, Figure S1E). Φ_{PSII} showed immediate and stark differences among treatments ($F_{(2,636)} = 113.44$, $P \ll 0.001$), which were sustained for nearly 2 months after the onset of warming, but then balanced out toward the end the experiment (i.e., weeks 8 and 10 of warming were not different, see Appendix S2; differences over time: $F_{(9,636)} = 11.06$, $P < 0.001$). Φ_{CO2} showed a similar trend being initially between 0.020 and 0.035 during the initial pre-treatment growth phase, but then measuring mostly between 0.010 and 0.025 by the end of the experimental warming phase (differences were significant over time: $F_{(9,636)} = 43.69$, $P \ll 0.001$ and among treatments: $F_{(2,636)} = 36.19$, $P \ll 0.001$). Differences in Φ_{CO2} among treatments persisted until week 7 of warming, then diminished (Appendix S2). Φ_{NPQ} was not different among treatments ($F_{(2,636)} = 1.431$, $P = 0.24$) exhibiting an increasing trend over time ($F_{(9,636)} = 186.43$, $P \ll 0.001$), ranging from 0.09 ± 0.02 during pretreatment to 0.33 ± <0.01 at the end of the experiment. The interaction of treatment and time was significant ($F_{(18,636)} = 7.624$, $P \ll 0.001$), leading to differences among treatments for the first 5 weeks of warming, then subsided, with treatments being similar at weeks 6, 8, and 9 of warming (Appendix S2). ETR_{PSII} measured 153.52 ± 1.56 µmol m^{-2} s^{-1} under pretreatment conditions, showed

maximum differences between treatments of roughly 75.76 μmol m^{-2} s^{-1} at week 9 to 11 (3 to 5 weeks after the onset of warming), with differences among temperature treatments equilibrating to around 112.97 ± 3.57 μmol m^{-2} s^{-1} thereafter (Appendix S2, weeks 8 and 10 of warming were not different). Again, differences were significant over time ($F_{(9,636)} = 11.96$, $P < 0.001$) and among treatments ($F_{(2,636)} = 137.92$, $P \ll 0.001$).

Before experimental warming, T_{opt} was between 29 and 30°C, and A_{opt} rates were > 20 μmol m^{-2} s^{-1}. Temperature optima for photosynthesis increased immediately (i.e., within 12 days of warming) and stabilized, with T_{opt} in both warming treatments settling around 33°C, and T_{opt} for the ambient treatment staying closer to 29°C (Table 2). Increases in T_{opt} and A_{opt} occurred faster in the +8°C treatment than in the +4°C treatment (Table 2, Figures 2 and S8), with A_{opt} peaking at 28 days of warming in the +8°C treatment (measuring 22.03 ± 0.62 μmol m^{-2} s^{-1}) but peaking at 41 days of warming for the +4°C treatment (measuring 20.44 ± 0.97 μmol m^{-2} s^{-1}, see Table S1 for *F* statistics). Over time, rates of A_{opt} displayed a similar divergent trend as rates of net photosynthesis from survey measurements (shown in Figure 1A), separating out by treatment, with the greatest differences coming 2 to 4 weeks after the initiation of the temperature treatments and then steadily declining (Figures 2 and S8). At that time, differences in A_{opt} were largest, and T_{opt} measured about 3°C greater in the two warming treatments than in the ambient treatment (Table 2). At the end of the warming experiment, T_{opt} was similar (i.e., within 0.6°C) for the two warming treatments, which were greater than the ambient treatment ($F_{(2,22)} = 42.28$, $P \ll 0.001$, Tables 2 and S2 and Figure S8). The net photosynthetic rate at 29°C ($A_{net,29}$, from photosynthetic-temperature response curves) between the ambient and +8°C treatment became statistically different at 28 days after warming began ($F_{(2,21)} = 4.83$, $P = 0.02$, Table S2). Differences in $A_{net,29}$ among treatments also emerged 55 days after warming began ($F_{(2,22)} = 3.70$, $P = 0.04$, Table S2). A_{opt} and $A_{net,29}$ showed a similar pattern, with no difference in rates at 41 days after the start of warming Table S2). However, differences between treatments emerged once more at 99 days because of a decrease in A_{opt} and $A_{net,29}$ in the ambient treatment (Tables 2 and S2 and Figure S8).

CO_2-response curves showed that there was a slight increase in the CO_2 compensation point of photosynthesis with increasing temperature and that rates of CO_2 assimilation at the compensation point increased (i.e., *A*-C_i curves shifted higher in the warmed treatments relative to the ambient treatment, Table 2, Figure S2). This change was most evident in the first 12 to 26 days following warming, wherein differences among treatments lessened as biochemical acclimation of photosynthesis to the increased temperatures occurred (Table S2). The result was that maximum rates of carboxylation ($V_{cmax,25}$) and electron transport ($J_{max,25}$) at 25°C decreased as plants matured during the initial establishment phase of the experiment, increased with warming, and then stabilized as leaf physiology acclimated to increased temperatures (Table 2 and Figure S8). For example, at 12 days after the start of the warming treatment, $J_{max,25}$ was greatest at 149.97 ± 6.72 μmol m^{-2} s^{-1} in the warmest treatment, being statistically greater than $J_{max,25}$ in the ambient and + 4°C treatments, which measured 109.93 ± 2.43 and 100.07 ± 5.09 μmol m^{-2} s^{-1}, respectively ($F_{(2,15)} = 24.43$, $P < 0.001$, Table 2). These differences in $J_{max,25}$ were statistically significant and remained so for about a month after warming began (28 days), then they equalized (Table S2 and Figure S8). $V_{cmax,25}$ increased and became more variable with the increasing temperature. Throughout the experiment, $V_{cmax,25}$ was 10–20 μmol m^{-2} s^{-1} greater in the warming treatment relative to the ambient treatment; however, these differences were no longer statistically significant after 1 month of warming (see Table S2 for *F*-statistics and Table 2 for Tukey HSD groupings).

Photosynthetic light response curves (Figure S4) showed a similar pattern in acclimation to the CO_2 response curves. Maximum rates of light-saturated photosynthesis (A_{max}) were different between at least two treatments for up to 28 days of warming (Table S3, see Table S4 or Appendix S2 for *F*-statistics). Differences in A_{max} among treatments reemerged at the end of the experiment, but only because A_{max} dropped substantially in the ambient treatment (Table S2 and Figure S8). The quantum yield of photosynthesis (Φ) exhibited an increasing then decreasing trend over time (which was statistically significant: $F_{(3,72)} = 31.683$, $P \ll 0.001$). Differences in Φ over time interacted with differences by treatment ($F_{(6,72)} = 2.728$, $P < 0.05$), which were greatest at 41 days after the start of the warming treatments, with Φ being lower in the warmest (+8°C) treatment relative to the ambient treatment ($F_{(2,72)} = 7.173$, $P < 0.001$), wherein differences in light curves among treatments equalized (Table S3 and Figure S4). Light compensation (I_{comp}) and light saturation ($I_{sat(75\%)}$) points were variable over time but generally tracked trends in photosynthetic acclimation (e.g., *A*, g_{sw}) across treatments (*F*-statistics were all significant, except for the interaction between treatment and time for $I_{sat(75\%)}$, see Appendix S2, Tables S3 and S4 and Figure S8).

3.2 | Acclimation of leaf dark respiration (R_d)

During the establishment period, leaf R_d rates at 29°C ($R_{d,29}$, from respiration-temperature response curves) were around 2.5 μmol m^{-2} s^{-1} and declined slightly as plants matured (Table 2, Table S2). $R_{d,29}$ was not statistically different among treatments ($F_{(2,74)} = 1.480$, $P = 0.24$), but was different over time ($F_{(3,74)} = 4.418$, $P = 0.007$), with a significant interaction between treatment and time ($F_{(6,74)} = 4.216$, $P = 0.001$). This led to differences in $R_{d,29}$ between treatments at 41 and 55 days after warming began (Tables 2 and S2 and Figure S8). Additionally, during the establishment period, the temperature sensitivity of R_d (Q_{10} R_d) was about 1.7 (Table 2, Figure 2). Leaf R_d acclimation lagged behind photosynthetic acclimation and seemed to be affected by the trimming of the plants, in that leaf $R_{d,29}$ rates were not different for the first month of warming (Table S2) but were depressed in the +8°C treatment after (Figures 2 and S8 and Tables 2 and S2). For instance, differences in $R_{d,29}$ were largest at 85 days (12 days after the start of the warming treatments), with depressed rates in the +8°C relative to the +4°C treatment (see Table 2 for Tukey HSD groupings). A decrease in $R_{d,29}$ of nearly 1 μmol m^{-2} s^{-1} occurred after trimming the plants (Table 2 and Figure S8). Patterns in leaf R_d at treatment temperature (as measured

TABLE 2 Leaf photosynthetic parameters over time

Treatment	Time	*N*	T_{opt} (°C)	A_{opt} (μmol m^{-2} s^{-1})	*Leaf* $R_{d,29}$ (μmol m^{-2} s^{-1})	Q_{10} R_d	$A_{net.29}$ (μmol m^{-2} s^{-1})	$V_{cmax,25}$ (μmol m^{-2} s^{-1})	$J_{max,25}$ (μmol m^{-2} s^{-1})
Initial	16 days	13	29.5 ± 0.2	24.38 ± 0.71	2.61 ± 0.09	1.82 ± 0.07	24.34 ± 0.71	97.21 ± 3.36	153.62 ± 4.66
Initial	39 days	7	29.7 ± 0.3	21.74 ± 0.97	2.52 ± 0.06	1.69 ± 0.07	20.50 ± 0.92	75.32 ± 1.88	114.07 ± 3.45
Ambient	56 days (12 days)	6	29.2 ± 0.3^{A}	18.51 ± 0.88^{A}	2.37 ± 0.13^{A}	1.79 ± 0.03^{A}	18.50 ± 1.00^{A}	71.87 ± 0.90^{A}	109.93 ± 2.43^{A}
+4°C		7	32.0 ± 0.3^{B}	17.55 ± 1.02^{A}	2.12 ± 0.15^{A}	1.80 ± 0.05^{A}	17.06 ± 1.00^{A}	71.46 ± 4.95^{A}	100.07 ± 5.09^{A}
+8°C		6	32.5 ± 0.3^{B}	20.13 ± 0.74^{A}	2.71 ± 0.21^{A}	1.71 ± 0.03^{A}	19.27 ± 1.00^{A}	89.26 ± 2.76^{B}	149.97 ± 6.72^{B}
Ambient	70 days (28 days)	9	29.2 ± 0.3^{A}	17.29 ± 0.76^{A}	2.18 ± 0.07^{A}	1.85 ± 0.09^{A}	17.26 ± 0.82^{A}	61.40 ± 3.19^{A}	84.86 ± 5.22^{A}
+4°C		8	32.1 ± 0.3^{B}	18.80 ± 0.74^{A}	1.76 ± 0.18^{A}	1.83 ± 0.17^{A}	18.22 ± 0.87^{AB}	63.78 ± 3.29^{A}	87.07 ± 5.03^{A}
+8°C		7	32.9 ± 0.7^{B}	22.03 ± 0.62^{B}	2.56 ± 0.40^{A}	1.61 ± 0.06^{A}	20.49 ± 0.87^{B}	77.59 ± 3.22^{B}	113.88 ± 6.37^{B}
Ambient	85 days (41 days)	6	30.4 ± 0.5^{A}	18.65 ± 1.07^{A}	1.89 ± 0.09^{AB}	1.97 ± 0.03^{A}	18.54 ± 1.00^{A}	61.41 ± 2.29^{A}	91.11 ± 4.24^{A}
+4°C		6	31.5 ± 0.2^{A}	20.44 ± 0.97^{A}	2.17 ± 0.17^{B}	1.90 ± 0.03^{A}	20.11 ± 1.00^{A}	66.88 ± 6.31^{A}	101.61 ± 12.55^{A}
+8°C		6	33.5 ± 0.3^{B}	19.67 ± 1.30^{A}	1.45 ± 0.08^{A}	1.85 ± 0.05^{A}	18.42 ± 1.00^{A}	71.81 ± 5.27^{A}	102.39 ± 7.84^{A}
Ambient	99 days (55 days)	6	28.1 ± 0.6^{A}	13.62 ± 1.14^{A}	2.31 ± 0.30^{B}	2.11 ± 0.09^{A}	13.52 ± 0.82^{A}	64.08 ± 7.35^{A}	90.28 ± 9.95^{A}
+4°C		8	33.2 ± 0.5^{B}	17.66 ± 0.94^{B}	1.90 ± 0.15^{AB}	1.90 ± 0.07^{A}	16.82 ± 0.93^{A}	54.16 ± 3.63^{A}	78.02 ± 6.10^{A}
+8°C		8	33.8 ± 0.2^{B}	17.88 ± 0.51^{B}	1.43 ± 0.06^{A}	1.97 ± 0.11^{A}	16.43 ± 0.82^{A}	69.93 ± 4.33^{A}	102.59 ± 5.29^{A}

Note: Mean values (±*SE*) for the temperature optimum of net photosynthesis (T_{opt}), the rate of net photosynthesis at T_{opt} (A_{opt}), the rate of dark respiration at 29°C (*Leaf* $R_{d,29}$), the temperature sensitivity of leaf dark respiration (Q_{10} R_d), the net rate of photosynthesis at 29°C ($A_{net,29}$), and Farquhar-Von Caemmerer-Berry model-derived estimates of the maximum carboxylation velocity at 25°C ($V_{cmax,25}$), and the maximum rate of electron transport at 25°C ($J_{max,25}$) by treatment, over time for *P. trichocarpa* clones. *N* denotes the number of physiological response curves used for parameter estimates. Numbers in parentheses in the Time column are the number of warmed days at the time of measurement. See Table S2 for ANOVA statistics ($n = 103$). Letters denote statistical groupings from Tukey HSD post-hoc tests; Tukey tests were done within each measurement time to account for repeated measures; thus, letters can only be compared among treatments within each time. For a visual representation of these data over time, see Figure S8.

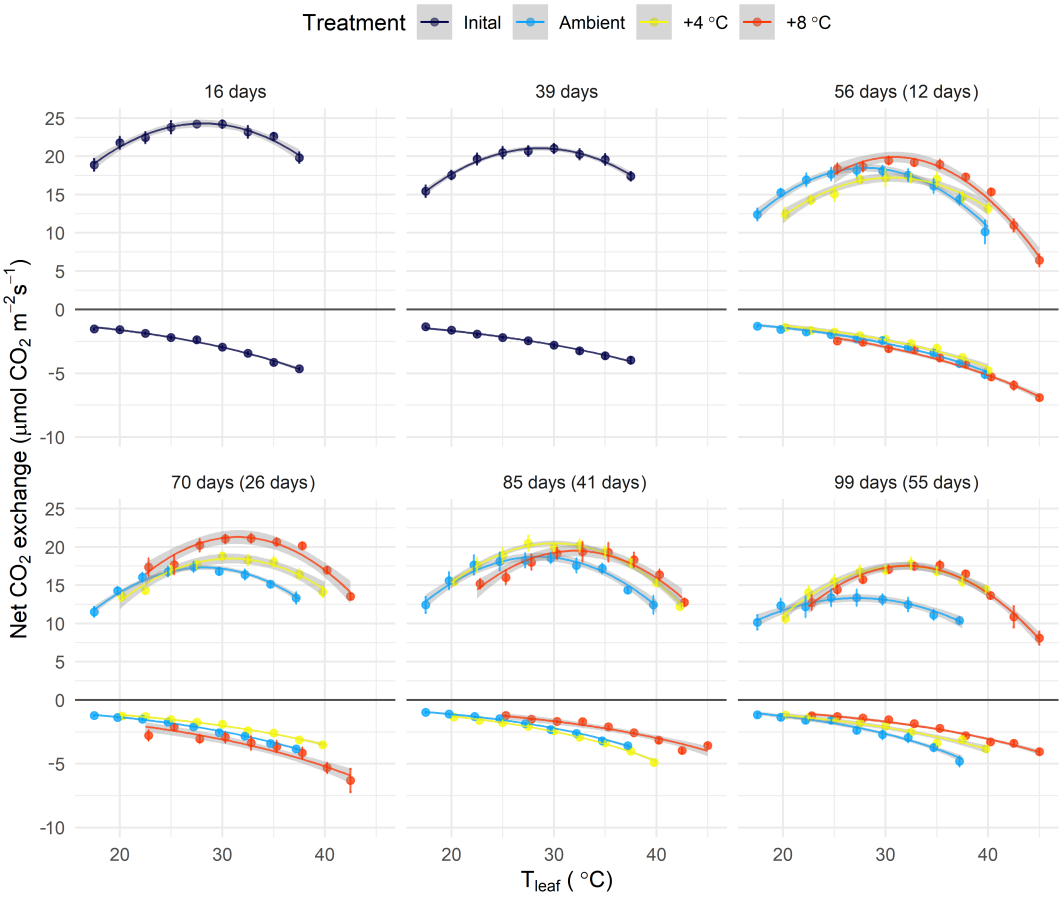

FIGURE 2 Temperature responses of leaf net CO_2 exchange over time for experimentally warmed *P. trichocarpa* clones. Values >0 are from photosynthesis-temperature response curves, while values <0 are from leaf dark respiration-temperature response curves. Points are means for at least six response curves, with bars showing standard errors. Lines are quadradic model fits for values >0 and exponential fits for values <0. Shading around lines shows 95% confidence intervals. Note the differences in the y-axis scale about zero. Photosynthesis and respiration temperature responses were measured on the same leaves (see Section 2). For fitted curves for each individual leaf see Figures S6 and S7. Note the differences in y-axis scale about zero. The number of days in parentheses indicates the number of warmed days at the time of measurement

during light response curves at 0 µmol m^{-2} s^{-1} light) showed a similar acclimation pattern to $R_{d,29}$, albeit less variable (Table S3 and Figure S8). R_d showed significant differences among treatments ($F_{(2,72)} = 11.52$, $P < 0.001$) and over time ($F_{(3,72)} = 13.07$, $P < 0.001$), with the interaction being significant (Tables S4 and S5, Appendix S2). Rates of leaf R_d always averaged <2 µmol m^{-2} s^{-1}, except for 12 days of warming in the +8°C treatment, and they were sometimes higher in warmed treatments than in the ambient treatment (Figure S8 see Table S3 for Tukey HSD groupings over time). Acclimation of R_d and $R_{d,29}$ reached homeostasis by 41 days of warming (day 85 of the experiment) in the +8°C treatment. In contrast, it continued to 55 days of warming (day 99) in the +4°C treatment (Figure 2, Tables 2 and S3, see and Figure S7 for individual leaf R_d-T response curves over time by treatment). Toward the end of the experiment (i.e., 55 days of warming), rates of $R_{d,29}$ were lowest in the +8°C treatment and highest in the ambient treatment (Table 2). ANOVA results for the temperature sensitivity of leaf dark respiration (Q_{10} R_d) showed differences among treatments ($F_{(2,73)} = 4.364$, $P = 0.02$) and over time ($F_{(3,743)} = 7.776$, $P < 0.001$), however these difference became marginally significant when the repeated measures error structure was incorporate into the ANOVA models (treatment: $F_{(2,10)} = 3.697$, $P = 0.06$, time: $F_{(3,15)} = 3.106$, $P = 0.06$, Appendix S2). Differences in Q_{10} R_d among treatments were greatest at 28 to 41 days after the start of the temperature treatments, with the differences being marginally significant ($P = 0.05$ and 0.09, respectively, Table S2, Appendix S2). By the end of the experiment (55 days after warming began), Q_{10} R_d was roughly 0.1–0.2 greater in the ambient treatment than in either of the warmed treatments (Table 2 and Figure S8).

3.3 | Variation in leaf morphology and nitrogen concentrations over time

Prior to pruning at week 10 (day 71) of the experiment, leaf morphologies were similar, with specific leaf area (SLA) values between 200 and 300 g cm^{-2} and leaf tissue N content between 3 and 4%. After plants were trimmed, leaf N content significantly decreased, dropping to below 3%, on average, in all treatments (Table S5 and Figure S8, also see Tukey HSD groupings and *F*-statistics in Table S6).

Leaf N content did not differ among treatments ($F_{(2,74)} = 0.517$, $P > 0.05$), but differed significantly over time ($F_{(3,74)} = 97.446$, $P < 0.001$), with the interaction of treatment and time being non-significant ($F_{(6,74)} = 1.435$, $P > 0.05$). These results were invariable to accounting for repeated measures error structure in the ANOVA (Appendix S2). There was a decrease in leaf C following plant trimming (time: $F_{(3,74)} = 45.948$, $P < 0.001$); prior to trimming, leaf C content was >45%, whereas leaf C content dropped to between 43 and 45% after plants were trimmed (Table S4). Leaf C content was also different among treatments ($F_{(2,74)} = 4.558$, $P < 0.05$), with the differences being greatest just before trimming at 28 days, after the beginning of the temperature treatments (Tables S5 and S6 and Figure S8). Similarly, SLA decreased significantly followed trimming (Table S6 and Figure S8, despite differences among treatments throughout the experiment, Table S5), as plants were forced to produce new stem and leaf biomass. Accordingly, the amount of leaf N per area (N_{area}) increased slightly, if not remaining the same (i.e., Tukey HSD groupings increased in certain cases after trimming like for the +4°C treatment, but did not in others, see Table S5). At the end of the experiment, whole-plant SLA, the ratio of the entire plant's leaf area to its leaf dry mass at the time of harvest, was statistically lower in the +4°C treatment than the ambient treatment ($F_{(2,48)} = 3.531$, $P < 0.05$), but was not different between the +4 and +8°C, or ambient and +8°C treatments (Table 5).

To evaluate if standardizing photosynthesis and respiration measurements by leaf N was necessary, we analyzed the relationships of leaf photosynthetic parameters (i.e., assimilation rates at 400 ppm from A-C_i curve fits, respiration rates at 0 μmol m^{-2} s^{-1} from light curves) to leaf N. Linear regressions showed that differences in Leaf N content affected leaf gas exchange variably among treatments (i.e., the slopes of the relationships of the leaf photosynthetic parameters to leaf N were statistically different, $P < 0.05$; see and Figure S3). Therefore, we standardized leaf temperature response curves by leaf N_{area}, and subtle differences emerged compared to the non-normalized temperature response curves (Figure 3). Leaf mass-N-based assimilation rates initially decreased in the warmer treatments, relative to the ambient treatments, before shifting their T_{opt} to warmer temperatures and increasing rates of photosynthesis at T_{opt} (Figure 3). For example, at 56 days (12 days after warming began), standardizing A by leaf N_{area} showed decreasing rates in the +8°C treatment relative to the other two treatments (Figure 3), whereas not accounting for leaf N_{area} showed that A increased in the +8°C treatment relative to the other two treatments (Figure 2). Similarly, at 70 days, standardizing A by leaf N_{area} decreased differences among the warmed treatments in A and R_d, and then, after plant trimming, standardizing A by leaf N_{area} revealed greater differences in A and R_d between treatments than for non-N standardized measurements (Figure 2 vs. Figure 3).

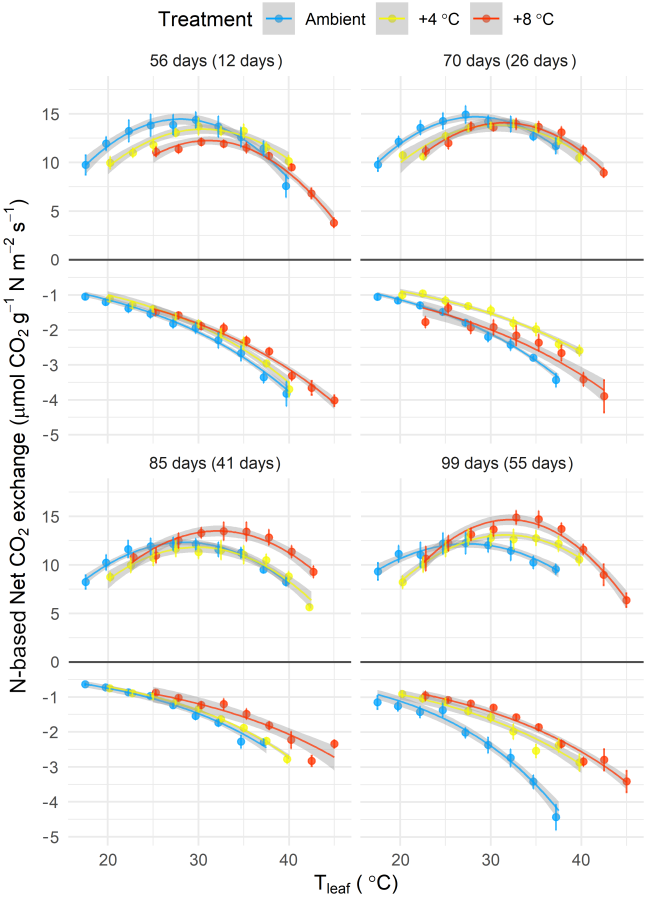

FIGURE 3 Temperature responses of N-based leaf net CO_2 exchange over time for *P. trichocarpa* clones starting after plants were introduced to experimentally-warmed conditions. These are the same data as Figure 2, except standardized by leaf N_{area} (in g cm^{-2}). Points are means for many response curves, with bars showing standard errors. Lines are quadradic model fits for values >0 and exponential fits for values <0. Shading around lines shows 95% confidence intervals. Note the differences in the y-axis scale about zero. The number of days in parentheses indicates the number of warmed days at the time of measurement

3.4 | Belowground soil CO_2 efflux

Rates of belowground CO_2 efflux (R_{BG}) were different by chamber, with chambers that had roots emitting about 1 μmol m^{-2} s^{-1} CO_2 more, on average, than chambers with soil only (β of 0.95 for the soil + roots, $P < 0.001$, Figures 1C, 4, and S9). During the initial establishment period, rates of soil CO_2 efflux (R_s) averaged 0.81 (± 0.05) μmol m^{-2} s^{-1} and rates of soil plus plant root CO_2 efflux (R_{s+r}) were 1.17 (± 0.07) μmol m^{-2} s^{-1}. The difference between R_{s+r} and R_s tended to increase as the plants established root biomass in the mesocosms (Figure 1C). Notably, R_{s+r} peaked after trimming the plants in week 11 of the experiment, then declined over the following several weeks (Figure 1C). The effect of time alone was only marginally significant in the LMM ($\beta = -0.03$, $P = 0.17$); however, the interaction of time with treatment was significant for both warmed treatments (both $\beta = 0.06$, $P < 0.05$), being slightly stronger for the +4°C than +8°C treatment, because of a greater difference in R_s and R_{s+r} in that treatment. During the 10-week warming period, rates of R_s were higher in the ambient than in the two warmed treatments, averaging 1.58 (±0.05) μmol m^{-2} s^{-1} in the ambient treatment and 1.07 (±0.06) and 1.04 (±0.07)

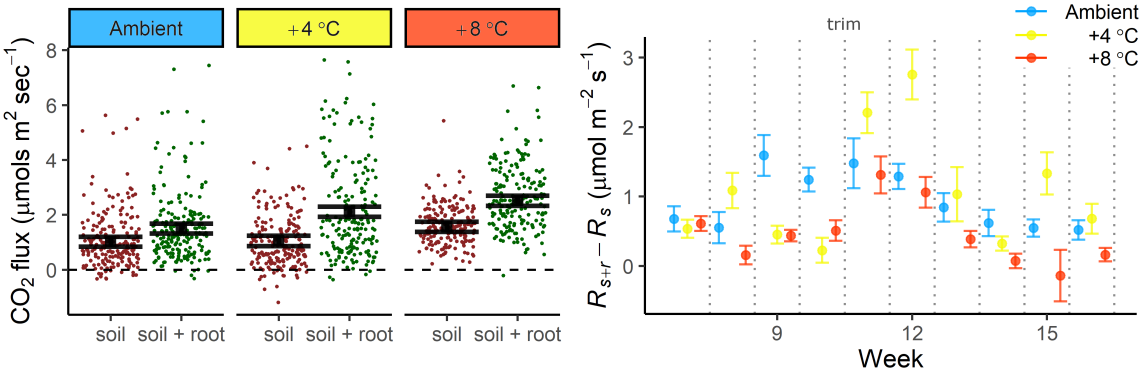

FIGURE 4 Belowground CO_2 flux (in µmol CO_2 per square meter soil area per second) from respiration collars within mesocosm growth boxes. Each box was divided into two portions (soil, R_s, and soil + root, R_{s+r}, see Figure 1C) using a 1-µ mesh barrier that prevented root growth into one-third of the mesocosm volume (see Section 2). Left: Average (±95% confidence intervals) for model predicted rates of belowground CO_2 flux for the 10-week warming period, where measurements were taken weekly. See Table 3 for belowground CO_2 flux Q_{10} values. Right: Mean (± *SE*) rates of root-associated belowground CO_2 flux, or the difference in soil plus root and soil only CO_2 release (R_{s+r} – R_s) for the 10 weeks of experimental warming. Note that plants were trimmed between weeks 10 and 11 (on day 71) of the experiment

µmol m^{-2} s^{-1} in the +4°C and + 8°C treatments, respectively (Figure 4). The LMM showed R_s to be significantly depressed in the two warmed treatments relative to the ambient treatment (β of −1.13 and −1.23 for the +4°C and +8°C treatments, respectively, $P < 0.001$, Figure S9 and Table S8). Rates of R_{s+r}, however, were depressed with increasing temperature, measuring 2.53 (±0.08), 2.14 (±0.11) and 1.52 (±0.08) µmol m^{-2} s^{-1} from the ambient to the +8°C treatment (Figures 4 and S9). The LMM showed that this was due to a significant negative interaction between treatment and chamber in the warmest +8°C treatment ($\beta = -0.47$, $P = 0.002$). The interaction between chamber and treatment was positive for the +4°C treatment (although non-significant, $\beta = 0.12$, $P = 0.44$, Figure S9 and Table S8).

Differences in R_s and R_{s+r} ($R_{s+r} - R_s$), or the net rates of belowground root-associated respiration, were higher on average and less variable in the ambient than in the two warming treatments (Figure 4). Two weeks into warming (i.e., at week 8 of the experiment), $R_{s+r} - R_s$ rates were higher in the +4°C treatment but lower in the +8°C treatment, relative to the ambient treatment (Figure 4). By the third week of warming, $R_{s+r} - R_s$ rates were similar in the two warming treatments, and to about half that of the rates measured in the ambient treatment. The trimming of plants at week 10 led to considerable increases in $R_{s+r} - R_s$ rates, with increases being greatest in the +4°C treatment (Figure 1C, Figure 4). In the weeks following the trim, $R_{s+r} - R_s$ rates declined in all treatments and then began to rebound around week 15 (Figure 4). $R_{s+r} - R_s$ rates were lowest in the +8°C treatment at the end of the experiment, with rates in the +4°C treatment being comparable to the ambient treatment. Net rates of belowground root-associated respiration during the 10-week warming period ($R_{s+r} - R_s$) were statistically different by treatment ($F_{(2,642)} = 20.074$, $P \ll 0.001$), and different over time ($F_{(9,642)} = 14.130$, $P \ll 0.001$), with a significant interaction between treatment and time ($F_{(18,642)} = 4.243$, $P < 0.001$, Figures 4 and 1C, Appendix S2). We measured the Q_{10} of R_{BG} using whole-plant temperature responses using the growth chambers, recording Q_{10} ranging from −0.34 to 2.74.

TABLE 3 The temperature sensitivity (Q_{10}) of belowground CO_2 efflux (R_{BG}). Q_{10} values are based on whole-plant temperature responses using the growth chambers (see Section 2)

Treatment	Chamber	Q_{10}
Ambient	Soil	0.539 ± 0.497^A
	Soil + root	0.649 ± 0.758^A
+4°C	Soil	0.582 ± 0.792^A
	Soil + root	0.666 ± 0.923^A
+8°C	Soil	0.493 ± 0.416^A
	Soil + root	0.285 ± 0.458^A
Treatment		$F_{(2,6)} = 0.224$
Chamber		$F_{(1,6)} = 0.393$
Treatment: Chamber		$F_{(2,6)} = 0.720$

Note: *F* statistics are for Analyses of Variance in the form of: ~Treatment × Chamber. *F* probabilities are all nonsignificant. Letters denote statistical groupings from Tukey HSD post-hoc tests ($n = 12$).

Means were not different by chamber or treatment (see Table 3 for means and *F*-statistics).

3.5 | Root tissue respiration

At the end of the experiment, root material was harvested from six plants per treatment to measure R_r-temperature responses. The temperature optima of R_r (T_{opt} R_r) were not statistically different among treatments ($F_{(2,15)} = 0.509$, $P > 0.05$), and all optima were between 45 and 46°C (Table 4). Mass-based respiration rates at temperature optima ($R_{r,opt}$) were about 10–20 µmol g^{-1} greater in the +4°C treatment than in either the +8°C or ambient treatments, and mass-based respiration rates 29°C ($R_{r,29}$) were about 10 µmol g^{-1} greater for the ambient treatment than for the warmed treatments; however, these differences were not statistically significant ($F_{(2,15)} = 0.215$, $P > 0.05$,

TABLE 4 Root respiration (R_r)–temperature response parameters

Treatment	T_{opt} R_r (°C)	Mass-based R_r		Mass N-based R_r		Q_{10} $R_{r,29}$
		$R_{r,opt}$ (μmol g^{-1} s^{-1})	$R_{r,29}$ (μmol g^{-1} s^{-1})	$R_{r-N,opt}$ (mmol g N^{-1} s^{-1})	$R_{r-N,29}$ (mmol g N^{-1} s^{-1})	
Ambient	45.40 ± 0.50^{A}	223.3 ± 18.6^{A}	145.5 ± 7.9^{A}	20.5 ± 2.2^{A}	12.8 ± 0.9^{A}	1.133 ± 0.004^{A}
+4°C	45.51 ± 0.22^{A}	241.5 ± 19.3^{A}	132.8 ± 11.1^{A}	19.5 ± 1.0^{A}	10.7 ± 0.6^{A}	1.143 ± 0.003^{AB}
+8°C	45.04 ± 0.26^{A}	229.1 ± 22.1^{A}	131.3 ± 14.3^{A}	15.6 ± 1.3^{A}	8.8 ± 0.7^{A}	1.153 ± 0.003^{B}
Treatment $F_{(2,15)}$	0.509	0.215	0.101	2.889$^{\$}$	2.134	9.906**

Note: Means ± *SE* for the temperature optimum of root reparation (T_{opt} R_r), the root respiration rate at T_{opt} ($R_{r,opt}$), the root respiration rate at 29°C ($R_{r,29}$), and the temperature sensitivity of root respiration at 29°C (Q_{10} $R_{r,29}$). Mass-based and mass N-based (-*N*) values are given (in μmol and mmol CO_2, respectively). *F*-statistics for analyses of variance in the form of: ~treatment. *F* probabilities are denoted as follows: **P < 0.01, $^{\$}P$ < 0.10 (i.e., is marginally significant). Letters denote statistical groupings from Tukey HSD post-hoc tests (n = 36). Note that the Q_{10} $R_{r,29}$ values for mass-based R_r and mass-N based R_r are equivalent, because for mass-N based measurements, the tissue CO_2 flux is divided by a constant—the root tissue N concentration.

Table 4). When R_r-temperature responses were standardized by root N content, $R_{r-N,opt}$ decreased with increasing temperature measuring 21, 20, and 16 mmol g^{-1} N s^{-1} from the ambient and two warming treatments, respectively. In this case, differences were marginally significant ($F_{(2,15)}$ = 2.889, P < 0.1). The temperature sensitivity of root respiration at 29°C (Q_{10} $R_{r,29}$), measured 1.113 ± 0.004 in the ambient treatment, 1.143 ± 0.003 in the +4°C treatment, and 1.153 ± 0.003 in the +8°C treatments. These differences were significant ($F_{(2,15)}$ = 9.906, P < 0.01), with the +8°C treatment being distinct from the ambient, but with the +4°C treatment being similar to them both (Table 4).

3.6 | Plant growth & biomass production

Statistical differences in plant growth and biomass occurred because of the experimental warming treatments. Plants grew taller in the two warmed treatments than in the ambient treatment (Table 5, $F_{(2,48)}$ = 31.09, P < 0.001). Basal diameter stem growth rates were greater in the +4°C treatment than in either the ambient or +8°C treatment (Table 5, $F_{(2,48)}$ = 5.88, P < 0.01). Similarly, leaf ($F_{(2,48)}$ = 26.29, P < 0.001), stem ($F_{(2,48)}$ = 14.43, P < 0.001), root ($F_{(2,48)}$ = 23.59, P < 0.001), and total biomass ($F_{(2,48)}$ = 31.39, P < 0.001) increments were all greater in the intermediate warming +4°C treatment than in the two other experimental treatments (Table 5, and Figure S5). Plants produced more leaf area ($F_{(2,48)}$ = 18.39, P < 0.001), and had greater belowground–aboveground (i.e., root to leaf plus shoot) allocation ratios ($F_{(2,48)}$ = 9.39, P < 0.01), in the +4°C treatment than in the two other treatments (Table 5). Allocation to roots was 20.50 ± 0.01% and 17.6 ± 0.01% in the ambient and + 8°C treatments, respectively, which was statistically different from the 26.20 ± 0.01% of biomass allocated to roots in the +4°C treatment (Table 5).

4 | DISCUSSION

We discuss our findings in three sections regarding the (1) aboveground acclimation (i.e., leaf photosynthesis and respiration), (2) belowground acclimation (i.e., root tissue respiration and soil respiration), and (3) growth response of *P. trichocarpa* to increased temperature over time.

4.1 | Aboveground acclimation of *P. trichocarpa* to warming

Acclimatory responses were similar in the two warmed treatments but occurred faster in the +8°C than in the +4°C treatment. This illustrates that there is a limit in the thermal acclimation capacity in *P. trichocarpa*. Photosynthetic acclimation to increased temperature showed an initial constructive adjustment (*sensu* Way & Yamori 2014), in that both A_{opt} and T_{opt} increased in the first 2 to 4 weeks of warming, but then A_{opt} decreased slightly as T_{opt} continued to increase in the +4 and + 8°C treatments (Figures 2 and S8). Based on comparing the differences in our leaf gas exchange measurements among treatments (Tables 2, S2–S4 and Figure S8), we can roughly characterize the acclimation of leaf gas exchange into two periods: the first month of warming (up to day 35 of warming to day 77 of the experiment), where acclimation was accelerating, and the second month or warming (from day 77 until the end of the experiment), where acclimation was stabilizing. Photosynthetic and respiratory acclimation to increased temperature was variable across individuals (Figures S6 and S7), likely because of small differences in environmental (e.g., light) conditions and inherent differences in the photosynthetic capacities of leaves. Yet, we found T_{opt} to be able to increase to near 34°C despite an air temperature increase of 8°C in our warmest treatment (Figures 2 and S8). This finding is similar to results from Weston et al. (2011), who reported that the temperature optimum of A_{max} for *P. trichocarpa* clones grown at 22°C was 32.6 ± 0.57°C, beyond which rates of photosynthesis decreased sharply.

Responses of T_{opt} and the A_{opt} were similar in both the +4 and +8°C treatments (Figures 2 and S8 and Table 2), leading us to conclude that there is a limitation on the ability of *P. trichocarpa* to physiologically acclimate to increased temperature. In theory, if there is no limit on photosynthetic acclimation, T_{opt} would increase twice as much in the +8°C treatment than the +4°C treatment, thus linearly

TABLE 5 Growth parameters (growth rates, biomass increments, allocation ratios, and whole-plant SLA—total plant leaf area divided by its dry weight) for *P. trichocarpa* plants grown in experimental conditions for the 16-week duration of the experiment ($n = 51$, with 17 per treatment, because some plants were harvested at various intervals during the experiment)

Treatment	Plant height growth (cm day^{-1})	Basal diameter growth rate (mm day^{-1})	Leaf biomass increment (g day^{-1})	Stem biomass increment (g day^{-1})	Root biomass increment (g day^{-1})	Total biomass increment (g day^{-1})	Leaf area increment (cm^2 day^{-1})	Belowground–aboveground allocation ratio	Whole-plant SLA (cm^2 g^{-1})
Ambient	2.30 ± 0.10^{A}	0.086 ± 0.005^{A}	0.46 ± 0.04^{A}	0.63 ± 0.06^{A}	0.23 ± 0.04^{A}	1.30 ± 0.13^{A}	83.0 ± 7.8^{A}	0.21 ± 0.01^{A}	182.4 ± 9.1^{B}
+4°C	2.83 ± 0.11^{B}	0.094 ± 0.004^{B}	0.77 ± 0.04^{B}	0.86 ± 0.07^{B}	0.43 ± 0.07^{B}	2.01 ± 0.12^{B}	125.5 ± 7.0^{B}	0.26 ± 0.01^{B}	163.2 ± 10.0^{A}
+8°C	2.89 ± 0.09^{B}	0.084 ± 0.004^{A}	0.55 ± 0.10^{A}	0.67 ± 0.08^{A}	0.22 ± 0.05^{A}	1.40 ± 0.18^{A}	90.9 ± 16.3^{A}	0.18 ± 0.01^{A}	176.6 ± 13.6^{AB}
Treatment $F_{(2,48)}$	30.83***	5.88**	26.29***	14.43**	23.59***	31.39***	18.39***	9.39***	3.531*

Note: The belowground–aboveground allocation ratio is the quotient of fresh root biomass to fresh leaf plus shoot biomass. Means ± 95% confidence intervals are presented, with letters denoting Tukey HSD statistical groupings of analysis of variance. *F*-statistics for Analyses of Variance in the form of ~Treatment. *F* probabilities are denoted as follows: *$P < 0.05$, **$P < 0.01$, and ***$P < 0.001$.

reflecting increases in air temperature. Similarly, lacking limitation on photosynthetic acclimation to warming, the constructive adjustments in A_{opt} would be twice as large in the +8°C treatment than the +4°C treatment. We observed maximum increases in T_{opt} of about 4°C, with similar responses in both warmed treatments despite a 4°C difference in temperature increase, supporting the existence of a limitation. Constructive adjustments in A_{opt} showed less limitation, in that the immediate constructive adjustment in A_{opt} (at 12 days after warming began) in the +8°C treatment was more than double that of the +4°C treatment. These differences attenuated over time with A_{opt} rates stabling near 18 μmol m^{-2} s^{-1} in both warming treatments by the end of the experiment (Figures 2 and S8), which is near the optimal photosynthetic rate of the species (Bassman & Zwier 1991).

Despite any limitation in the magnitude of photosynthetic acclimation, acclimation occurred more rapidly in the +8°C treatment relative to the +4°C treatment. Not only did increases in T_{opt} lag increases in air temperature, but the greater the increase in air temperature, the more T_{opt} lagged, suggesting that the increase in T_{opt} with increasing air temperatures might take the form of a saturating curve. Considering our results and the similarity in responses between the +4 and +8°C treatment, we suggest that increase T_{opt} likely saturates near 29°C (i.e., +4°C ambient air temperature in our experiment). We do show, however, that *P. trichocarpa* can increase the thermal optimum of photosynthesis by about two degrees but may be physiologically limited to acclimate further. Indeed, a shift in T_{opt} of two degrees is consistent with the consensus in the literature that it can shift by one-third to half of the magnitude of change in air temperatures (Kumarathunge et al. 2019; Sage & Kubien 2007). A 33% increase in T_{opt} in our case would be 1.3 and 2°C for the +4 and + 8°C treatments, respectively; Similarly, a 50% increase in T_{opt} would be 2.7 and 4°C. Net average increases in T_{opt} over 55 days of warming maximized at 4.3°C, being similar among both warming treatments at about 4°C (Table 2) and demonstrating limitation to increase beyond 4°C.

Warming also led to a significant increase in stomatal conductance (g_{sw}, Figure 1B). Increases in g_{sw} reflected increased photosynthetic rates at growth temperatures, which is a principal criterion for acclimation (Way & Yamori 2014). Maintaining similar *A* with a decline in g_{sw} with warming suggests a combination of adjusting both leaf water loss and inherit photosynthetic capacity to maintain leaf carbon balance at a higher temperature (Berry & Björkman 1980; Sage & Kubien 2007). We measured g_{sw} near 1 mol m^{-2} s^{-1} in our warmest treatment during the first month of acclimation (Figure 1B). Similarly, Bassman and Zwier (1991) reported rates of g_{sw} of up to 1 μmol m^{-2} s^{-1}, with some variation across poplar varieties because of susceptibility to water stress. In contrast, Zhang et al. (1999) reported g_{sw} values that averaged 0.271 (±0.013) mol m^{-2} s^{-1}, accounting for seasonal and diurnal variation from mature *P. trichocarpa* trees growing in the floodplain of the Thames River in southeastern England. Thus, the high rates of stomatal conductance we measured are likely because plants were young and leaves were in a developmental stage, optimizing carbon gain over water loss. Additionally, high rates of stomatal conductance help reduce leaf

temperature via transpirative cooling; thus, increasing g_{sw} is likely a strategy poplar leaves use to cope with high temperatures. Stomatal conductance initially decreased during the first week of warming, increased sharply in the following weeks, and then decreased to become similar across treatments (Figure 1B). Although temperature effects on g_{sw} are considered indirect (i.e., they are mediated by vapor pressure deficit or evapotranspiration; Urban et al. 2017) and vary widely across leaves and individual trees, an initial, short-term reduction of g_{sw} in response to temperature stress has been documented in other temperate C_3 trees, like red maple (Weston & Bauerle 2007).

Increased rates of photosynthesis were driven, in part, by adjustments in the light-capturing reactions and biochemical mechanics of photosynthesis (Tables 2, S2, and S4, and Figures S1, S4, and S8). This is consistent with previous research in that both the kinetics of electron transport in photosystems (i.e., light reactions) and the enzyme-catalyzed biochemical (i.e., carbon) reactions of the Calvin cycle in C_3 photosynthesis have been shown to increase with temperature and then adjust their rates of reaction (i.e., acclimate) with time (Bernacchi et al. 2003; Berry & Björkman 1980; Von Caemmerer 2000; Yamasaki et al. 2002). We observed more rapid and slightly greater increases in estimates of $J_{max,25}$ and $V_{cmax,25}$ in the +8°C treatment than in the +4°C treatment (Figure S8), as well as more rapid and greater changes in chlorophyll fluorescence parameters in the +8°C treatment than in the +4°C treatment (Figure S1). Additionally, we observed an increase in leaf N_{area} with increasing temperature (Tables S5 and S6 and Figure S8). This increase was affected by (i.e., did not persist after) trimming of the plants. Increased leaf N_{area} could be related to (1) upregulation of photosynthetic enzyme (e.g., Rubisco) production and use, (2) increased soil N availability due to higher mineralization rates at higher temperatures, resulting in increased plant uptake, and/or (3) an increased demand for N to maintain growth, respiration and photosynthesis at higher temperatures (i.e., as T_{opt} shifts toward greater T and A-C_i and leaf R_d curves shift upward).

These findings together show that both the light and carbon reactions of photosynthesis adjusted to increased temperatures (Tables 2 and S2 and Figures S3 and S8). The increase in chlorophyll fluorescence signifies greater light stress, in that either the downstream carbon reactions of photosynthesis are limiting the use of captured light energy, or there was a decrease in the quantum efficiency of photosystem photochemistry (Briantais et al. 1996). However, after acclimation occurred during the second month of warming, the magnitude of change in $J_{max,25}$, $V_{cmax,25}$, T_{opt}, and A_{opt}, was similar in both the +4°C and + 8°C treatments (Table 2), potentially signifying a physiological limitation on the degree of thermal acclimation of photosynthesis in the poplar plants studied. We base this conclusion on the observation that despite double the magnitude of thermal stress in the warmest treatment relative to the intermediate warming treatment, adjustments in most photosynthetic parameters were of similar magnitude across both warming treatments. Differences in photosynthetic rates among treatments were greatest at 12 to 26 days post warming, and then photosynthetic rates became more similar, demonstrating that thermal acclimation of photosynthesis can occur in poplar in days to weeks (Tables 2 and S2, and Figures 3 and S4).

Acclimation of leaf respiration occurred in concert with the acclimation of photosynthesis to warming. By 41 to 55 days of warming, the acclimation of R_d was stabilizing, with $R_{d,29}$ rates increasing in warmed treatments during the first month of warming to measure >2 μmol m^{-2} s^{-1}, and then dropping down below 2 μmol m^{-2} s^{-1} in the second month of warming (Figures 3, S7, and S8 and Table 2). The thermal sensitivity of leaf respiration, Q_{10} R_d, showed little variability among treatments (i.e., differences were never significant among treatments at any single time point), ranging between 1.6 and 2.1 μmol m^{-2} s^{-1}, indicating that the shape of leaf R_d–temperature relationships were largely unaffected because of acclimation of R_d rates to higher temperatures (Tables 2, S2, and Figures 2, S7, S8). When Q_{10} R_d is unaffected in the acclimation of respiration, it suggests that the acclimation is being driven by a change in the elevation and not the slope of the temperature-respiration relationship. This is consistent with type II acclimation of R_d (Atkin et al. 2005, *sensu* Atkin & Tjoelker 2003).

4.2 | Acclimation of soil CO_2 efflux and belowground acclimation of poplar to warming

Belowground physiological acclimation to warming is much more difficult to measure repeatedly over time than aboveground acclimation. We found only minimal differences in root respiration, R_r, at the end of the experiment, which were moderated by root N content. Among treatments, warming led to a decrease in soil respiration, R_s, of roughly one-third (Table 3 and Figure 4). All belowground respiration Q_{10} values were <1 (Table 3), indicating that heterotrophic R_s decreased with increasing temperature. In a meta-analysis on the temperature sensitivity of belowground respiration, R_{BG}, Li et al. (2020) found that root tissues increase the Q_{10} values of R_{BG} (i.e., increase the temperature sensitivity of soil CO_2 efflux), likely because heterotrophic R_s decreases but R_r increases with increasing temperature. Qualitatively consistent with those findings, our results from the whole-chamber temperature response showed that when roots were present in soil, we measured slightly greater Q_{10} values of belowground respiration in the ambient and +4°C treatments than when roots were absent (i.e., growth medium alone; Table 3). These differences were not significant, however, likely because of low levels of replication (n=12, two per each respiration chamber per treatment) relative to the magnitude of respiratory change in the plant-soil experimental system. We completed the whole-plant temperature responses using the growth chambers twice and replicating more would have decreased the variability in our R_{BG} Q_{10} estimates. Yet, for the +8°C treatment, the Q_{10} value for R_{s+r} was about half that of R_s, providing some observational evidence that in the warmest treatment, R_{s+r} had a greater reduction in respiration rate than R_s alone (Table 3). R_{s+r} was 16% lower in the +4°C treatment versus ambient temperature, and 28% lower in the +8°C treatment versus +4°C treatment, and this variation is likely due to differences in heterotrophic (i.e., microbial) and not autotrophic (i.e., root-related) R_{BG}. Indeed, R_r did not vary systematically across treatments (Table 4, Figure 5), but R_s was statistically

distinct in the two warmed treatments relative to the ambient treatment (Table S8, Figures 4 and S9). Jarvi and Burton (2013) reported an increase in R_{BG} with *in situ* experimental warming of *Acer saccharum* dominated soils, with R_r showing partial, soil moisture-mediated acclimation, and R_s increasing in warmed plots due to increased N-mineralization rates. The difference we observed between R_{s+r} and R_s was largest in the +4°C treatment, potentially illustrating a belowground temperature optimum for the plant–soil system, where heterotrophic metabolism of plant-derived liable C is greatest (Figure 4). We observed large increases in R_{S+r} (i.e., plant-associated R_{BG}) after trimming the plants (Figure 4), and these increases were largest in the +4°C treatment, potentially showing how the poplar plants in that treatment allocated the greatest amount of liable C to belowground to mine N for new leaf and stem tissue production (Melillo et al. 2011). The greater ability of plants to access N in the +4°C treatment than the other two treatments likely led to the differences observed in plant growth and biomass production.

Regarding root tissue respiration, R_r averaged between 130 and 150 μmol g^{-1} s^{-1} at 29°C for *P. trichocarpa*, with substantial variation among the root systems of individual plants (Figure S10). $R_{r,29}$ values were slightly but not significantly lower and more variable in the warmed treatments than in the ambient treatment; however, those differences were accentuated (becoming marginally significant) when we standardized by root N content ($R_{r-N,29}$, Table 4 and Figure 5). In agreement with several studies (Ceccon et al. 2016; Noh et al. 2020; Reich et al. 2008), standardizing R_r rates by tissue N content helped constrain variation among individuals (Figures S11 and S12) because root tissue N is an important indicator of root metabolic activity due to its involvement with ion uptake, and root protein and enzyme function. Although $R_{r-N,29}$ was not different among treatments (Table 4), R_{r-N} at higher temperatures was depressed in the +8°C treatment relative to the two other treatments (Figure 5), pointing to the important role that tissue N content has in relation to R_r. Thus, we found clear differences in the temperature sensitivity of root respiration at 29°C (Q_{10} $R_{r,29}$, Table 4), with the warmest +8°C treatment having a greater sensitivity than the ambient treatment. Due to the lower tissue N content of the plants grown in +8°C treatment relative to the two other treatments, the R_{r-N}-temperature relationship was shifted lower. The Q_{10} of R_r was depressed at lower temperatures (i.e., between 10 and 20°C) in the ambient treatment relative to the two warmed treatments, potentially illustrating the effect of thermal acclimation on increasing rates of R_r at lower temperatures (i.e., a broadening of the R_r Q_{10}-temperature relationship Figure 5).

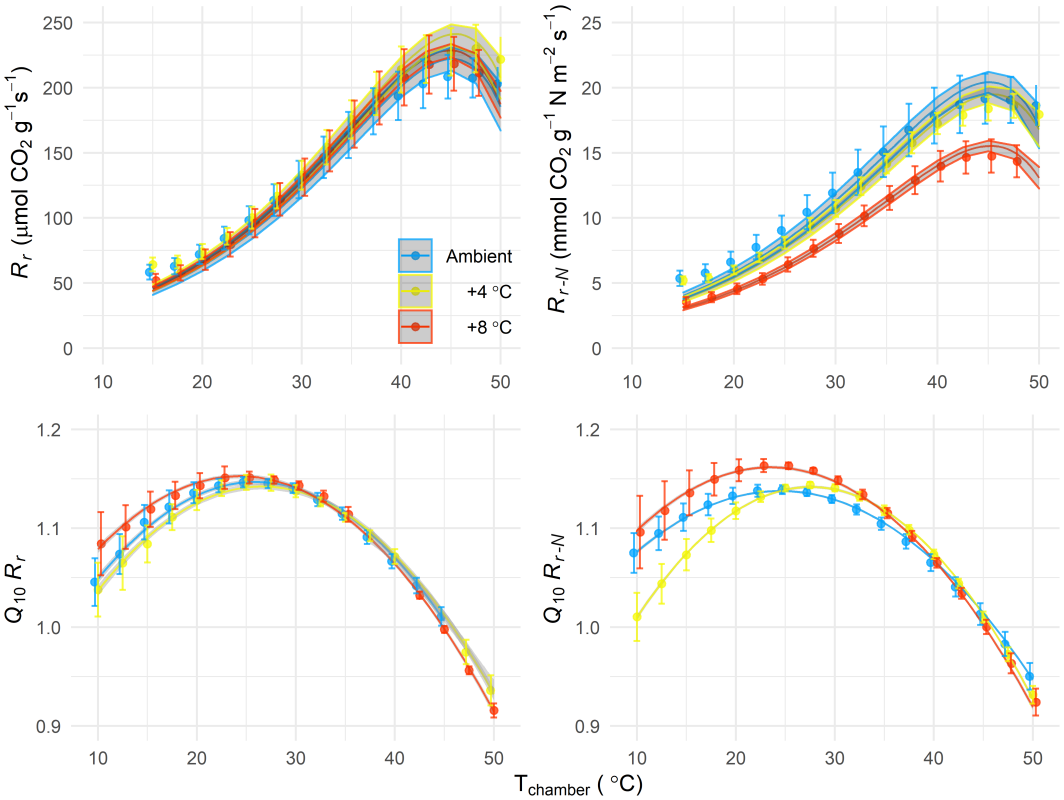

FIGURE 5 Mass-based root respiration rate (R_r), mass-N-based root respiration rate (R_{r-N}) and their temperature sensitivities (bottom panels) by treatment for experimentally warmed *P. trichocarpa* clones. R_r – T response curves were measured at the end of the experiment (at 94 and 109 days) on six root systems per treatment (see Figures S11 and S12 for curves by individual root tissue samples). Points are means (±*SE*), and shaded areas show 95% confidence intervals for model fits. The R_r – T curves were fit using an exponential model. Because R_r Q_{10} varies with T (Palta & Nobel 1989), R_r Q_{10} was calculated at each T by differentiating a fitting third-order polynomial curve to log-transformed R_r data (see Atkin et al. 2000). Finally, a quadratic model was fit to the R_r Q_{10} – T curves (shown in bottom panels)

Severe temperature stress likely requires higher plant N utilization, which can result in an N-dilution effect (Jarrell & Beverly 1981). For example, warming has been shown to decrease the N content and increase lipid content in algal tissues (Converti et al. 2009). However, the dilution effect of temperature on tissue N contents depends on the relative temperature sensitivity of active and passive N uptake, soil N metabolism, N diffusion and mass flow, and microbial and plant N enzyme kinetics in the soil (Jarrell & Beverly 1981; Jarvi & Burton 2013). These processes can all potentially increase with warming as well. For example, warming-induced soil carbon losses were compensated by plant carbon (i.e., root biomass) gains, which were driven by increased N-availability in an ecosystem warming experiment at Harvard Forest, Massachusetts (Melillo et al. 2011). Thus, increased N availability and utilization by plants with warming can affects plant-soil carbon dynamics through the production of new roots. Generally, the relative contribution of respiration in roots to ion uptake and root growth decreases with root system age, while the relative contribution of respiration to the maintenance of root biomass increases (Bouma 2005; Jarvi & Burton 2018; van der Werf et al. 1988). For example, R_r was substantially different for established root systems (5 weeks and 2 years old) versus rain-produced roots (1 week and 6 weeks old) in *Agave desertii* (Palta & Nobel 1989). Similar results have been reported for poplar, with rates of root respiration decreasing by about 50% by 3 weeks of age (Ceccon et al. 2016). Root system age-related changes in metabolic activity, and hence R_r, might explain some of the temporal variation in R_{s+r} and $R_{s+r} - R_s$ (Figure 1C, Figure 4). Nevertheless, because the root tissues used for the root respiration-temperature response curves were all about the same age (94–109 days old), tissue age likely had little effect on the R_r-temperature response curves. Based on the assumption that roots were established, being roughly 3 months old but still being metabolically active, we can infer that the majority (i.e., at least half) of root tissue respiration stemmed from biomass maintenance, with the other half being partitioned between root ion uptake and growth (Ceccon et al. 2016). Additionally, we can assume that differences in root N content were a function of N re-translocation to aboveground biomass production, leading to more of a dilution effect in the $+4^{\circ}$C treatment, where more stem and leaf biomass was produced after trimming; however, this was variable among plants (Table S7 and Figure S5).

4.3 | The growth response of poplar to warming

Striking differences in plant biomass production resulted because of temperature. Biomass production was greatest for the intermediate temperature treatment, evidencing a thermal optimum in growth temperature for the species near 29°C. Considering the widespread distribution and cultivation of poplars throughout North America (Kutsokon et al. 2015; Wullschleger et al. 2002), perhaps the starkest results of this experiment were the differences in plant biomass production (Table 5). Plant biomass production was greatest at intermediate warming (i.e., 29°C daytime temperature and 25°C nighttime temperature), with total biomass increment being nearly 50% greater, root biomass increment having doubled, stem biomass being one-third greater, and leaf biomass being 40–67% greater at intermediate warming than at the other two temperatures (Table 5 and Figure S5). The native range for *P. trichocarpa* is primarily from northern California to southeastern Alaska, experiencing a variable climate (DeBell 1990). The *Nisqually-1* clone used in this project was initially collected in riparian temperate forest of western Washington state. Using plantation yield data from 23 countries, Kutsokon et al. (2015) found that poplar plantation productivity was positively correlated with yearly temperature and the number of hot days during the growing season, albeit weakly and with some variation due to the cultivation method and poplar variety. Our results demonstrate that although there is some benefit to increased temperatures for biomass production, that benefit is limited, especially at higher temperatures, where the physiological cost of acclimation (in both C and N economics) outweighs any increase in carbon gain via photosynthesis. Although leaf respiration did acclimate, warming led to its increase initially (Figures 2, 3, and S10 and Tables 2 and S2). R_{s+r} rates were depressed in the warmest $+8^{\circ}$C treatment (Figure 4), as was N-based R_r. (Figure 5). The initial increase in leaf and whole plant respiration results in a C cost, which coupled with the N cost of photosynthetic adjustment likely drives decreased C and N economic margins at the whole plant-scale. Collectivelty, this results in decreased allocation to roots, labile C release belowground and depressed R_{BG}, which could have futher ecosystem feedbacks in a natural system.

The native range of *P. trichocarpa* has been warming and will continue to warm as anthropogenic climate change persists and intensifies (Hansen et al. 2010). Like many of the trees in the Salicaceae, *P. trichocarpa* requires large amounts of water to thrive (Théroux Rancourt et al. 2015), and there have even been efforts to improve the water use efficiency of the species to conserve water use in agricultural settings (Kalluri et al. 2020). A single, small poplar tree of about 5 cm stem diameter and 6 m height can transpire over 25 L of water in a given day, taking a significant portion (between 10 and 60%) of its water from the groundwater table (Zhang et al. 1999). We found that evaporation plus transpiration was 41% and 73% greater at $+4$ and $+8^{\circ}$C, respectively, than for mesocosms at ambient conditions. Although the plants in our experiment were not water-limited, temperature stress and subsequent acclimation *in situ* rarely occur in this context. Therefore, photosynthetic and respiratory acclimation to increased temperatures will likely be dependent on water availability for wild or plantation-grown poplar trees (Broeckx et al. 2014). The increase in g_{sw} associated with thermal acclimation results in increased water loss, which is an important consideration to take into account because the effects of global climate change often couple warming with increased variability in precipitation and increasing drought frequency (Allen et al. 2015; McDowell et al. 2020).

5 | CONCLUSIONS

All else being equal (i.e., given adequate water and nutrients), *P. trichocarpa* can physiologically acclimate to increased temperatures,

although we find that the aboveground acclimatory response was restricted to a shift in the photosynthetic temperature optimum (T_{opt}) of 2–3°C. Both C and N economies potentially limit physiological acclimation with consequences for reduced plant growth, especially when thermal stress is severe. Whole plant N-economics plays a fundamental role in the acclimatory response, as changes in the reaction kinetics of key proteins (e.g., RuBP, Rubisco) involved in photosynthesis underpin leaf acclimation and drive the physiological cost of acclimation. Concerning leaf C-economics, constructive adjustments in photosynthesis were underpinned by higher rates of electron transport (J_{max}) and carboxylation (V_{cmax}), which persisted for up to about 1 month after the start of warming, then stabilized to background levels. We found that generally, belowground CO_2 release reflected patterns in aboveground CO_2 assimilation, illustrating a linkage in plant C economics through the plant–soil system as acclimation occurred.

Belowground, we found that rates of root respiration showed some minor differences among temperature treatments (e.g., in their thermal sensitivities of respiration and in respiration rates at the extremes of the temperature range), indicating some ability to acclimate to thermal stress. Notably, there were clear plant biomass production differences among treatments, with aboveground biomass having been stimulated in both warmed treatments, but root biomass reaching its maximum at +4°C warming, with at least 5% more biomass allocated to roots. Thus, there appears to be some limitation in the magnitude of physiological acclimation in *P. trichocarpa*, with moderate warming (i.e., a few to several degrees C) resulting in increased productivity up to a point, whereafter productivity declines. Our results show that photosynthetic acclimation can occur within a month, whereas belowground acclimation and the consequences of the cost of the acclimation at the plant- and ecosystem-scale likely take longer to develop. Environmental warming occurs in concert with other stressors, such as pathogens or drought. Although our results point to the ability of *P. trichocarpa* to acclimate to, or even benefit from, predicted future temperature conditions, field studies of forest and plantation trees are needed to corroborate our experimental findings and to determine if the results presented here indicate responses of wild or plantation-grown trees of *P. trichocarpa* or other poplar species.

ACKNOWLEDGMENTS

We thank Lionel Perez-Collazo, David McLennan, Keith van Schaick, and Zach Ziegler for help with measurements and plant harvests. We also thank Will Cook at the Duke Environmental Isotope laboratory for his assistance with the nutrient analysis. We thank Dr. Zoran Bursac and the personnel of the FIU Statistics Department for statistical advice. We are grateful to Martijn Slot for discussions and for providing helpful feedback on the manuscript. This material is based upon work supported by the U.S. Department of Energy, Office of Science, Office of Workforce Development for Teachers and Scientists, Office of Science Graduate Student Research (SCGSR) program, and by Office of Biological and Environmental Research. The SCGSR program is administered by the Oak Ridge Institute for Science and Education (ORISE) for the DOE. ORISE is managed by ORAU under contract number DE-SC0014664. ORNL is managed by UT-Battelle, LLC, for the DOE under contract DE-AC05-1008 00OR22725. All opinions expressed in this paper are the author's and do not necessarily reflect the policies and views of DOE, ORAU, or ORISE.

AUTHORS CONTRIBUTIONS

J. Aaron Hogan and Jeffrey M. Warren conceived research plans, Jeffrey M. Warren, Miranda D. Clark, and David J. Weston supervised the experiments, J. Aaron Hogan performed the experiments using methods developed by Cari Ficken; Miranda D. Clark provided technical assistance to J. Aaron Hogan; J. Aaron Hogan analyzed the data and wrote the article with contributions of all the authors; Christopher Baraloto and Jeffrey M. Warren advised, Jeffrey M. Warren supervised and completed the writing. J. Aaron Hogan agrees to serve as the author responsible for contact and ensures communication.

DATA AVAILABILITY STATEMENT

Data and metadata are archived on the webpage of Oak Ridge National Laboratory Terrestrial Ecosystem Science Scientific Focus Area: Hogan et al. (2020) https://doi.org/10.25581/ornlsfa.018/1617459.

ORCID

J. Aaron Hogan https://orcid.org/0000-0001-9806-3074
Christopher Baraloto https://orcid.org/0000-0001-7322-8581
Cari Ficken https://orcid.org/0000-0003-4132-4354
Miranda D. Clark https://orcid.org/0000-0002-4839-1309
David J. Weston https://orcid.org/0000-0002-4794-9913
Jeffrey M. Warren https://orcid.org/0000-0002-0680-4697

REFERENCES

Adams, M.A., Buckley, T.N. & Turnbull, T.L. (2020) Diminishing CO_2-driven gains in water-use efficiency of global forests. *Nature Climate Change*, 10, 466–471.

Aitken, S.N., Yeaman, S., Holliday, J.A., Wang, T. & Curtis-McLane, S. (2008) Adaptation, migration or extirpation: climate change outcomes for tree populations. *Evolutionary Applications*, 1, 95–111.

Allen, C.D., Breshears, D.D. & McDowell, N.G. (2015) On underestimation of global vulnerability to tree mortality and forest die-off from hotter drought in the Anthropocene. *Ecosphere*, 6, 1–55.

Atkin, O.K., Bruhn, D. & Tjoelker, M.G. (2005) Response of plant respiration to changes in temperature: mechanisms and consequences of variations in Q_{10} values and acclimation. In: Lambers, H. & Ribas-Carbo, M. (Eds.) *Plant respiration: from cell to ecosystem*. Dordrecht, Netherlands: Springer, pp. 95–135.

Atkin, O.K., Edwards, E.J. & Loveys, B.R. (2000) Response of root respiration to changes in temperature and its relevance to global warming. *The New Phytologist*, 147, 141–154.

Atkin, O.K. & Tjoelker, M.G. (2003) Thermal acclimation and the dynamic response of plant respiration to temperature. *Trends in Plant Science*, 8, 343–351.

Bassman, J.H. & Zwier, J.C. (1991) Gas exchange characteristics of *Populus trichocarpa*, Populus deltoides and *Populus trichocarpa* × *P. deltoides* clones. *Tree Physiology*, 8, 145–159.

Bates, D., Mächler, M., Bolker, B. & Walker, S. (2015) Fitting linear mixed effects models using lme4. *Journal of Statistical Software*, 67(1), 1–48.

Bernacchi, C., Pimentel, C. & Long, S.P. (2003) In vivo temperature response functions of parameters required to model RuBP-limited photosynthesis. *Plant, Cell & Environment*, 26, 1419–1430.

Berry, J. & Björkman, O. (1980) Photosynthetic response and adaptation to temperature in higher plants. *Annual Review of Plant Physiology*, 31, 491–543.

Bond-Lamberty, B. & Thomson, A. (2010) Temperature-associated increases in the global soil respiration record. *Nature*, 464, 579–582.

Bouma, T.J. (2005) Understanding plant respiration: separating respiratory components versus a process-based approach. In: Lambers, H. & Ribas-Carbo, M. (Eds.) *Plant respiration: from cell to ecosystem*. Dordrecht, Netherlands: Springer, pp. 177–194.

Briantais, J.-M., Dacosta, J., Goulas, Y., Ducruet, J.-M. & Moya, I. (1996) Heat stress induces in leaves an increase of the minimum level of chlorophyll fluorescence, Fo: a time-resolved analysis. *Photosynthesis Research*, 48, 189–196.

Broeckx, L.S., Verlinden, M.S. & Ceulemans, R. (2014) Seasonal variations in photosynthesis, intrinsic water-use efficiency and stable isotope composition of poplar leaves in a short-rotation plantation. *Tree Physiology*, 34, 701–715.

Bryla, D., Bouma, T., Hartmond, U. & Eissenstat, D. (2001) Influence of temperature and soil drying on respiration of individual roots in citrus: integrating greenhouse observations into a predictive model for the field. *Plant, Cell & Environment*, 24, 781–790.

Burton, A., Pregitzer, K., Ruess, R., Hendrick, R. & Allen, M. (2002) Root respiration in North American forests: effects of nitrogen concentration and temperature across biomes. *Oecologia*, 131(4), 559–568.

Canham, C.D., Murphy, L., Riemann, R., McCullough, R. & Burrill, E. (2018) Local differentiation in tree growth responses to climate. *Ecosphere*, 9, e02368.

Ceccon, C., Tagliavini, M., Schmitt, A.O. & Eissenstat, D.M. (2016) Untangling the effects of root age and tissue nitrogen on root respiration in *Populus tremuloides* at different nitrogen supply. *Tree Physiology*, 36, 618–627.

Chapin, F.S., III, McFarland, J., McGuire, A.D., Euskirchen, E.S., Ruess, R. W. & Kielland, K. (2009) The changing global carbon cycle: linking plant-soil carbon dynamics to global consequences. *Journal of Ecology*, 97, 840–850.

Converti, A., Casazza, A.A., Ortiz, E.Y., Perego, P. & Del Borghi, M. (2009) Effect of temperature and nitrogen concentration on the growth and lipid content of Nannochloropsis oculata and *Chlorella vulgaris* for biodiesel production. *Chemical Engineering and Processing*, 48, 1146–1151.

Crous, K.Y., Drake, J.E., Aspinwall, M.J., Sharwood, R.E., Tjoelker, M.G. & Ghannoum, O. (2018) Photosynthetic capacity and leaf nitrogen decline along a controlled climate gradient in provenances of two widely distribued eucalyptus species. *Global Change Biology*, 24, 4626–4644.

Cunningham, S. & Read, J. (2002) Comparison of temperate and tropical rainforest tree species: photosynthetic responses to growth temperature. *Oecologia*, 133, 112–119.

DeBell DS (1990) *Populus trichocarpa* Torr. & Gray. Black cottonwood. In: Burms RM, Honkala BH *Silvics of North America, Vol. 2, Hardwoods, Agriculture Handbook 654*. Washington DC: United States Department of Agriculture (USDA) Forest Service, pp. 570–576.

Dusenge, M.E., Duarte, A.G. & Way, D.A. (2019) Plant carbon metabolism and climate change: elevated CO_2 and temperature impacts on photosynthesis, photorespiration and respiration. *The New Phytologist*, 221, 32–49.

Duursma, R.A. (2015) Plantecophys-an R package for analysing and modelling leaf gas exchange data. *PLoS One*, 10, e0143346.

Eissenstat, D., McCormack, M.L. & Du, Q. (2013) Global change and root lifespan. In: Eschel, A. & Waisel, Y. (Eds.) *Plant roots: the hidden half*. 4th: CRC Press, pp. 399–412.

Farquhar, G.D., von Caemmerer, S.V. & Berry, J.A. (1980) A biochemical model of photosynthetic CO_2 assimilation in leaves of C3 species. *Planta*, 149, 78–90.

Feeley, K.J., Rehm, E.M. & Machovina, B. (2012) Perspective: the responses of tropical forest species to global climate change: acclimate, adapt, migrate, or go extinct? *Frontiers of Biogeography*, 4, 69–82.

Ficken, C.D. & Warren, J.M. (2019) The carbon economy of drought: comparing respiration responses of roots, mycorrhizal fungi, and free-living microbes to an extreme dry-rewet cycle. *Plant and Soil*, 435, 407–422.

García-Carreras, B., Sal, S., Padfield, D., Kontopoulos, D.-G., Bestion, E., Schaum, C.-E. et al. (2018) Role of carbon allocation efficiency in the temperature dependence of autotroph growth rates. *Proceedings of the National Academy of Sciences of the United States of America*, 115, E7361–E7368.

Gornall, J.L. & Guy, R.D. (2007) Geographic variation in ecophysiological traits of black cottonwood (*Populus trichocarpa*). *Botany*, 85, 1202–1213.

Hansen, J., Ruedy, R., Sato, M. & Lo, K. (2010) Global surface temperature change. *Reviews of Geophysics*, 48, RGR4004.

Heberling, J.M. & Fridley, J.D. (2013) Resource-use strategies of native and invasive plants in eastern north American forests. *The New Phytologist*, 200, 523–533.

Heskel, M.A., O'Sullivan, R.P.B., Tjoelker, M.G., Weerasinghe, L.K., Penilland, A., JJG, E. et al. (2016) Convergence in the temperature response of leaf respiration across biomes and plant functional types. *Proceedings of the National Academy of Sciences of the United States of America*, 113, 3832–3837.

Hikosaka, K. (1997) Modelling optimal temperature acclimation of the photosynthetic apparatus in C3 plants with respect to nitrogen use. *Annals of Botany London*, 80, 721–730.

Hikosaka, K., Ishikawa, K., Borjigidai, A., Muller, O. & Onoda, Y. (2005) Temperature acclimation of photosynthesis: mechanisms involved in the changes in temperature dependence of photosynthetic rate. *Journal of Experimental Botany*, 57, 291–302.

Hogan, J.A., Baraloto, C., Ficken, C.D., Clark, M.D., Weston, D.M. & Warren, J.M. (2020) *Physiological responses of Populus trichocarpa to warming*. Oak Ridge, Tennessee, USA: Oak Ridge National Laboratory, TES SFA, U.S. Department of Energy. https://doi.org/10.25581/ornlsfa.018/1617459

IPCC. (2014) Climate change 2014 synthesis report-summary for policymakers. In: Core Writing Team, Pachauri, R.K. & Meyer, L.A. (Eds.) *Intergovernmental panel on climate change (IPCC)*. Geneva, Switzerland: IPCC, p. 151.

Jarrell, W.M. & Beverly, R.B. (1981) The dilution effect in plant nutrition studies. In: Brandy, N.C. (Ed.), Vol. 34. Advances in Agronomy, pp. 197–224.

Jarvi, M.P. & Burton, A.J. (2013) Acclimation and soil moisture constrain sugar maple root respiration in experimentally warmed soil. *Tree Physiology*, 33, 949–959.

Jarvi, M.P. & Burton, A.J. (2018) Adenylate control contributes to thermal acclimation of sugar maple fine-root respiration in experimentally warmed soil. *Plant, Cell & Environment*, 41, 504–516.

Jump, A.S. & Peñuelas, J. (2005) Running to stand still: adaptation and the response of plants to rapid climate change. *Ecology Letters*, 8, 1010–1020.

Kalluri, U.C., Yang, X. & Wullschleger, S.D. (2020) Plant biosystems design for a carbon-neutral bioeconomy. *Biodesign Research*, 2020, 7914051.

King, A.W., Gunderson, C.A., Post, W.M., Weston, D.J. & Wullschleger, S. D. (2006) Plant respiration in a warmer world. *Science*, 312, 536–537.

Kumarathunge, D.P., Medlyn, B.E., Drake, J.E., Tjoelker, M.G., Aspinwall, M.J., Battaglia, M. et al. (2019) Acclimation and adaptation components of the temperature dependence of plant photosynthesis at the global scale. *The New Phytologist*, 222, 768–784.

Kutsokon, N., Jose, S. & Holzmueller, E. (2015) A global analysis of temperature effects on populus plantation production potential. *American Journal of Plant Sciences*, 6, 23–33.

Kuznetsova, A., Brockhoff, P.R. & Christensen, R.H.B. (2017) LmerTest package: tests in linear mixed effects models. *Journal of Statistical Software*, 82(13), 1–26.

Lambers, H., Atkin, O.K. & Millenaar, F.F. (1996) Respiratory patterns in roots in relation to their functioning. In: Eschel, A. & Waisel, Y. (Eds.) *Plant roots: the hidden half*, Vol. 3, New York, NY: Marcel Dekker Inc., pp. 521–552.

Larson, P.R. & Isebrands, J. (1971) The plastochron index as applied to developmental studies of cottonwood. *Canadian Journal of Forest Research*, 1, 1–11.

Li, J., Pendall, E., Dijkstra, F.A. & Nie, M. (2020) Root effects on the temperature sensitivity of soil respiration depend on climatic condition and ecosystem type. *Soil and Tillage Research*, 199, 104574.

Lombardozzi, D.L., Bonan, G.B., Smith, N.G., Dukes, J.S. & Fisher, R.A. (2015) Temperature acclimation of photosynthesis and respiration: a key uncertainty in the carbon cycle-climate feedback. *Geophysical Research Letters*, 42, 8624–8631.

Luo, Y. (2007) Terrestrial carbon–cycle feedback to climate warming. *Annual Review of Ecology, Evolution, and Systematics*, 38, 683–712.

Marshall, B. & Biscoe, P. (1980) A model for C3 leaves describing the dependence of net photosynthesis on irradiance. *Journal of Experimental Botany*, 31, 29–39.

Mathias, J.M. & Thomas, R.B. (2021) Global tree water use efficiency is enhanced by increased atmospheric CO_2 and modulated by climate and plant functional types. *Proceedings of the National Academy of Sciences of the United States of America*, 118, e2014286118.

McDowell, N.G., Allen, C.D., Anderson-Teixeira, K., Aukema, B.H., Bond-Lamberty, B., Chini, L. et al. (2020) Pervasive shifts in forest dynamics in a changing world. *Science*, 368, eaaz9463.

McMahon, S.M., Parker, G.G. & Miller, D.R. (2010) Evidence for a recent increase in forest growth. *Proceedings of the National Academy of Sciences of the United States of America*, 107, 3611–3615.

Melillo, J.M., Butler, S., Johnson, J., Mohan, J., Steudler, P., Lux, H. et al. (2011) Soil warming, carbon-nitrogen interactions, and forest carbon budgets. *Proceedings of the National Academy of Sciences of the United States of America*, 108, 9508–9512.

Monleon, V.J. & Lintz, H.E. (2015) Evidence of tree Species' range shifts in a complex landscape. *PLoS One*, 10, e0118069.

Moore, C.E., Meacham-Hensold, K., Lemonnier, P., Slattery, R.A., Benjamin, C., Bernacchi, C.J. et al. (2021) The effect of increasing temperature on crop photosynthesis from enzymes to ecosystems. *Journal of Experimental Botany*, earab090. 72, 2822–2844.

Noh, N.J., Kristine, C., Jinquan, L., Zineb, C., Craig, B., Stefan, A. et al. (2020) Does root respiration in Australian rainforest tree seedlings acclimate to experimental warming? *Tree Physiology*, 40, 1192–1204.

Palta, J.A. & Nobel, P.S. (1989) Root respiration for *Agave deserti*: influence of temperature, water status and root age on daily patterns. *Journal of Experimental Botany*, 40, 181–186.

Peñuelas, J., Canadell, J.G. & Ogaya, R. (2011) Increased water-use efficiency during the 20th century did not translate into enhanced tree growth. *Global Ecology and Biogeography*, 20, 597–608.

Pregitzer, K.S., King, J.S., Burton, A.J. & Brown, S.E. (2000) Responses of tree fine roots to temperature. *The New Phytologist*, 147, 105–115.

Pregitzer, K.S., Laskowski, M.J., Burton, A.J., Lessard, V.C. & Zak, D.R. (1998) Variation in sugar maple root respiration with root diameter and soil depth. *Tree Physiology*, 18, 665–670.

R Core Team. (2019) *R: a language and environment for statistical computing*. Vienna, Austria: R Foundation for Statistical Computing.

Reich, P.B., Tjoelker, M.G., Pregitzer, K.S., Wright, I.J., Oleksyn, J. & Machado, J.L. (2008) Scaling of respiration to nitrogen in leaves, stems and roots of higher land plants. *Ecology Letters*, 11, 793–801.

Reich, P.B., Walters, M., Tjoelker, M., Vanderklein, D. & Buschena, C. (1998) Photosynthesis and respiration rates depend on leaf and root morphology and nitrogen concentration in nine boreal tree species differing in relative growth rate. *Functional Ecology*, 12, 395–405.

Rogers, A., Kumarathunge, D.P., Lombardozzi, D.L., Medlyn, B.D., Serbin, S.P. & Walker, A.P. (2020) Triose phosphate utilization limitation: an unnecessary complexity in terrestial biosphere model representation of photosynthesis. *New Phytologist*, 230, 17–22.

Roumet, C., Birouste, M., Picon-Cochard, C., Ghestem, M., Osman, N., Vrignon-Brenas, S. et al. (2016) Root structure-function relationships in 74 species: evidence of a root economics spectrum related to carbon economy. *The New Phytologist*, 210, 815–826.

Sage, R.F. & Kubien, D.S. (2007) The temperature response of C3 and C4 photosynthesis. *Plant, Cell & Environment*, 30, 1086–1106.

Scafaro, A.P., Xiang, S., Long, B.M., Bahar, N.H.A., Weerasinghe, L.K., Creek, D. et al. (2017) Strong thermal acclimation of photosynthesis in tropical and temperate wet-forest tree species: the importance of altered Rubisco content. *Global Change Biology*, 23, 2783–2800.

Sharkey, T.D. (2019) Is triose phosphate utilization important for understanding photosynthesis? *Journal of Experimental Botany*, 70, 5521–5525.

Silim, S.N., Ryan, N. & Kubien, D.S. (2010) Temperature responses of photosynthesis and respiration in *Populus balsamifera* L.: acclimation versus adaptation. *Photosynthetic Research*, 104, 19–30.

Slot, M. & Kitajima, K. (2015) General patterns of acclimation of leaf respiration to elevated temperatures across biomes and plant types. *Oecologia*, 177(3), 885–900.

Slot M, Winter K (2016) The effects of rising temperature on the ecophysiology of tropical forest trees. In: Santiago LS, Goldstein G (eds.) *Tropical tree physiology*. Switzerland: Springer International Publishing, pp. 385–412.

Smith, N.G. & Dukes, J.S. (2013) Plant respiration and photosynthesis in global-scale models: incorporating acclimation to temperature and CO_2. *Global Change Biology*, 19, 45–63.

Smith, N.G., Li, G. & Dukes, J.S. (2019) Short-term thermal acclimation of dark respiration is greater in non-photosynthetic than in photosynthetic tissues. *AoB Plants*, 11, plz064.

Smith, N.G., McNellis, R. & Dukes, J.S. (2020) No acclimation: instantaneous responses to temperature maintain homeostatic photosynthetic rates under experimental warming across a precipitation gradient in *Ulmus americana*. *AoB Plants*, 12, plaa017.

Song, Y., Chen, Q., Ci, D., Shao, X. & Zhang, D. (2014) Effects of high temperature on photosynthesis and related gene expression in poplar. *BMC Plant Biology*, 14, 111.

Théroux Rancourt, G., Éthier, G. & Pepin, S. (2015) Greater efficiency of water use in poplar clones having a delayed response of mesophyll conductance to drought. *Tree Physiology*, 35, 172–184.

Urban, J., Ingwers, M., McGuire, M.A. & Teskey, R.O. (2017) Stomatal conductance increases with rising temperature. *Plant Signaling & Behavior*, 12, e1356534.

van der Werf, A., Kooijman, A., Welschen, R. & Lambers, H. (1988) Respiratory energy costs for the maintenance of biomass, for growth and for ion uptake in roots of Carex diandra and *Carex acutiformis*. *Physiologia Plantarum*, 72, 483–491.

von Caemmerer, S. (2000) *Biochemical models of leaf photosynthesis*. Victoria, Australia: Csiro Publishing.

Walther, G.-R. (2003) Plants in a warmer world. *Perspectives in Plant Ecology*, 6, 169–185.

Wang, J., Dufrenne, C., McCormack, M.L., Yang, L., Tian, D., Luo, Y. et al. (2021) Fine-root functional trait response to experimental warming: a global meta-analysis. *New Phytologist*, 230, 1856–1867.

Way, D.A. & Yamori, W. (2014) Thermal acclimation of photosynthesis: on the importance of adjusting our definitions and accounting for thermal acclimation of respiration. *Photosynthetic Research*, 119, 89–100.

Weston, D.J. & Bauerle, W.L. (2007) Inhibition and acclimation of C3 photosynthesis to moderate heat: a perspective from thermally contrasting genotypes of *Acer rubrum* (red maple). *Tree Physiology*, 27, 1083–1092.

Weston, D.J., Karve, A.A., Gunter, L.E., Jawdy, S.S., Yang, X., Allen, S.M. et al. (2011) Comparative physiology and transcriptional networks underlying the heat shock response in *Populus trichocarpa*, Arabidopsis thaliana and *Glycine max*. *Plant, Cell & Environment*, 34, 1488–1506.

Wullschleger, S.D., Jansson, S. & Taylor, G. (2002) Genomics and forest biology: Populus emerges as the perennial favorite. *Plant Cell*, 14, 2651–2655.

Yamasaki, T., Yamakawa, T., Yamane, Y., Koike, H., Satoh, K. & Katoh, S. (2002) Temperature acclimation of photosynthesis and related changes in photosystem II electron transport in winter wheat. *Plant Physiology*, 128, 1087–1097.

Yamori, W., Hikosaka, K. & Way, D.A. (2014) Temperature response of photosynthesis in C 3, C 4, and CAM plants: temperature acclimation and temperature adaptation. *Photosynthesis Research*, 119, 101–117.

Yamori, W., Suzuki, K., Noguchi, K., Nakai, M. & Terashima, I. (2006) Effects of Rubisco kinetics and Rubisco activation state on the temperature dependence of the photosynthetic rate in spinach leaves from contrasting growth temperatures. *Plant, Cell & Environment*, 29, 1659–1670.

Zhang, H., Morison, J.I. & Simmonds, L.P. (1999) Transpiration and water relations of poplar trees growing close to the water table. *Tree Physiology*, 19, 563–573.

SUPPORTING INFORMATION

Additional supporting information may be found online in the Supporting Information section at the end of this article.

How to cite this article: Hogan, J.A., Baraloto, C., Ficken, C., Clark, M.D., Weston, D.J. & Warren, J.M. (2021) The physiological acclimation and growth response of *Populus trichocarpa* to warming. *Physiologia Plantarum*, 1–22. Available from: https://doi.org/10.1111/ppl.13498